AD-A097 821 CALIFORNIA INST OF TECH PASADENA F/G 9/1
LOW LOSS FLEXIBLE DIELECTRIC WAVEGUIDE FOR MILLIMETER-WAVE TRAN--ETC(U)
MAR 81 W B BRIDGES N00014-79-C-0839
UNCLASSIFIED SRO-0005-1 NL

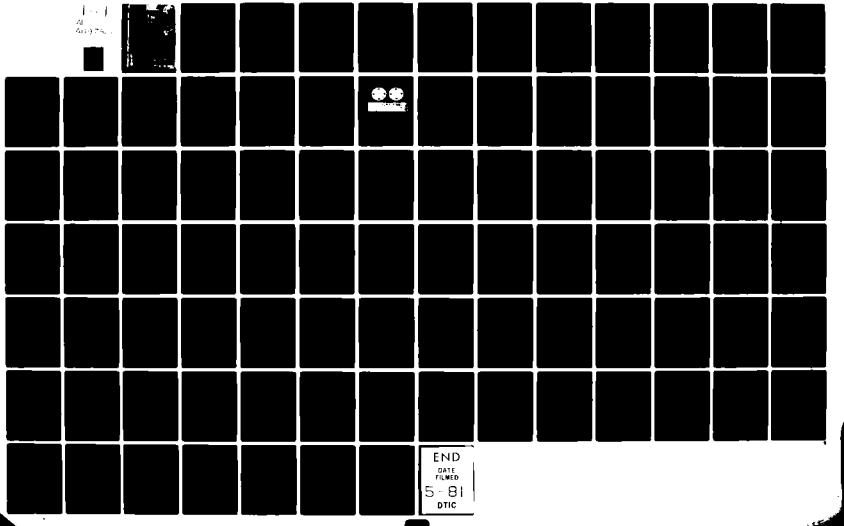

END
DATE FILMED
5-81
DTIC

AD A097821

[illegible]

Annual [illegible]

[illegible]

Contract [illegible]

Project [illegible]

William B. Bridges – Principal Investigator

Reporting Period: 1 September 19[illegible]

Prepared for Office of Naval Research [illegible]

[illegible]

UNCLASSIFIED

SECURITY CLASSIFICATION OF THIS PAGE (When Data Entered)

REPORT DOCUMENTATION PAGE	READ INSTRUCTIONS BEFORE COMPLETING FORM
1. REPORT NUMBER: SRO-005-1	2. GOVT ACCESSION NO.: AD-A097 822
3. RECIPIENT'S CATALOG NUMBER	
4. TITLE (and Subtitle): Low-Loss Flexible Dielectric Waveguide for Millimeter-Wave Transmission and its Application to Devices	5. TYPE OF REPORT & PERIOD COVERED: Annual Technical 9/1/79 to 11/8/80
	6. PERFORMING ORG. REPORT NUMBER: ONR 81-1
7. AUTHOR(s): William B. Bridges	8. CONTRACT OR GRANT NUMBER(s): N00014-79-C-0839
9. PERFORMING ORGANIZATION NAME AND ADDRESS: California Institute of Technology, 116-81 Pasadena, California 91125	10. PROGRAM ELEMENT, PROJECT, TASK AREA & WORK UNIT NUMBERS: 61153N RR 021-02-03
11. CONTROLLING OFFICE NAME AND ADDRESS: Office of Naval Research Code 427 Arlington, VA 22217	12. REPORT DATE: March 1981
	13. NUMBER OF PAGES: 90
14. MONITORING AGENCY NAME & ADDRESS(if different from Controlling Office)	15. SECURITY CLASS. (of this report): UNCLASSIFIED
	15a. DECLASSIFICATION/DOWNGRADING SCHEDULE

16. DISTRIBUTION STATEMENT (of this Report)
Approved for public release; distribution unlimited

17. DISTRIBUTION STATEMENT (of the abstract entered in Block 20, if different from Report)

18. SUPPLEMENTARY NOTES
ONR Scientific Officer: Tel. (202) 696-4218

19. KEY WORDS (Continue on reverse side if necessary and identify by block number)
millimeter-waves
dielectric waveguides
dielectric loss
dielectric constant
loss tangent
KRS-5
KRS-6

20. ABSTRACT (Continue on reverse side if necessary and identify by block number)
Dielectric properties have been measured at 94 GHz for thallium halide materials KRS-5 and KRS-6 using Fabry-Perot resonance transmission and short-waveguide reflection in dielectric-filled waveguide sections. The dielectric constants are 31-32 for KRS-5 and 28-31 for KRS-6; the loss tangents are 2 x 10^{-2} for both. These values predict a waveguide loss of 8 dB/cm for a closely-confined HE_{11} mode in KRS-5 at 94 GHz. Difficulties in coupling to such high dielectric constant fibers have so far prevented

DD FORM 1 JAN 73 1473 EDITION OF 1 NOV 65 IS OBSOLETE
S/N 0102-LF-014-6601

UNCLASSIFIED
SECURITY CLASSIFICATION OF THIS PAGE (When Data Entered)

direct measurement, but scale model studies at 10 GHz yield a successful coupling technique to the HE_{11} mode through an intermediate dielectric.

Propagation in a 0.5 mm diameter KRS-5 fiber was observed with 0.2 dB/cm loss, much lower than that predicted for HE_{11}; the as-yet unidentified mode has a phase velocity about c, but small external fields and less than 1.5 dB loss from a 90°, 20 cm radius bend. Propagation constants for KRS-5 waveguides were calculated and losses estimated for various designs. A loosely coupled HE_{11} KRS-5 fiber with foamed-teflon cladding could exhibit 3 dB/meter loss, with 3 dB/meter additional loss from 60 cm radius bends. A simple theory of relative guiding properties for multilayer cylindrical waveguides is given.

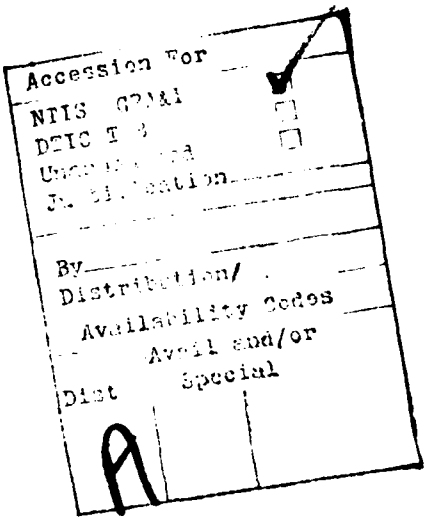

CALIFORNIA INSTITUTE OF TECHNOLOGY

Pasadena, California

(12) 89

(6)

Low Loss Flexible Dielectric Waveguide for Millimeter-Wave Transmission and its Application to Devices

Annual Technical Report SRO-0005-1 (16) RR021102

on

(15) Contract N00014-79-C-0839 (17) RR021102,03

Project Number SRO-005

(14) SRO-0005-1, 81-1-ONR

(10) William B. Bridges - Principal Investigator

(9) Annual technical repti

Reporting Period: 1 Sep[illegible] 1979 - 1 Nov[illegible] 1980,

Prepared for Office of Naval Research, Code 427

Arlington VA 22217 (11) Mar 81

071550

This report covers research performed under contract N00014-79-0839 at the California Institute of Technology, Pasadena, California 91125 and, under subcontract, at the Hughes Research Laboratories, Malibu, California 90265 for the first year of this three year program, 1 September 1979 through 1 November 1980.

Personnel contributing to this work were:

William B. Bridges, Professor of Electrical Engineering and Applied Physics, Caltech; Principal Investigator (213) 356-4809.

Marvin B. Klein, Member of the Technical Staff, Hughes Research Labs, Co-principal Investigator (213) 456-6411 X247.

Arthur E.-T. Chiou, Graduate Student, Caltech (213) 356-4848.

Reynold E. Johnson, Senior Associate Engineer, Hughes Research Labs, (213) 456-6411 X173.

Phyllis R. Nelson, Graduate Student, Caltech (213) 356-4853.

Edgard Schweig, Graduate Student, Caltech (213) 356-4854.

The authors of each section of the report are identified at the beginning of the section.

TABLE OF CONTENTS

I. INTRODUCTION AND SUMMARY (W. B. Bridges)

A. Background

A few years ago, workers at the Hughes Research Laboratories (Ref. I-1) developed an extrusion process for drawing long poly-crystalline fibers of the mixed crystal thallium bromide-thallium iodide, known as KRS-5 in the infrared community. The original motivation for their work was to develop a transmission medium for infrared sources, particularly the 10 micron CO_2 laser, that would have low loss analogous to the glass optical fibers at visible and near IR wavelengths. Further studies indicated that KRS-5 fibers were, indeed, suitable for 10 micron transmission, and that the theoretical losses should be incredibly low, orders of magnitude less than those already obtained for glass fibers. The Hughes work on KRS-5 for IR transmission continues under another program.

The availability of fibers in sizes up to 0.5 mm diameter stimulated Popa and Johnson at Hughes to measure the properties of this material for its potential as a dielectric waveguide at millimeter wavelengths (Ref. I-2). The initial measurements were encouraging (although in retrospect their dielectric constant value turns out to be wrong):

1. a loss tangent of 2.3×10^{-3} and a dielectric constant of 19 were measured at 35 GHz in a short dielectric-filled waveguide resonator;
2. significant transmission was observed (but not measured quantitatively) through a 2 meter section of KRS-5 fiber at 94 GHz with simple coupling sections in and out; further, the bending losses seemed small, since the transmission changed little even with loops in the fiber of less than 0.5 meter radius

As a result of this work we decided to undertake a joint program between Caltech and Hughes to further assess the potential of KRS-5 and other materials that were being drawn by the Hughes process (e.g., KRS-6) for their use as a practical dielectric waveguide transmission medium at millimeter wavelengths; we also wished to investigate possible device applications that employ evanescent wave coupling to a low loss transmission medium. The present program under ONR sponsorship is the result, and this report covers the progress made under the first year of a three year effort.

B. Summary and Results

During this past year, several tasks were undertaken in parallel. The results obtained to date are summarized here.

1. Measurements of the bulk dielectric properties of KRS-5 and KRS-6 were made using two different dielectric-filled metallic waveguide techniques at 94 GHz and at 10 GHz. We find that the dielectric constant of KRS-5 at 94 GHz is 31-32, essentially the same as the value at low frequencies. The loss tangent of KRS-5 is 2×10^{-2} at 94 GHz. The corresponding numbers for KRS-6 are 28-31 and 2×10^{-2}. Teflon and Rexolite samples were also measured with the same techniques to serve as controls on the methods. The results of these measurements have been submitted for publication (Ref. I-3); a preprint is contained as Section II of this report.

2. An open Fabry-Perot resonator technique capable of measuring low-loss materials was investigated, and preliminary measurements were made on samples of Rexolite. However, the results of the waveguide measurements indicate that the loss in KRS-5 is not low enough to warrant the use of this technique.

3. Dielectric waveguide measurements were attempted at 94 GHz on 0.5 mm and 0.4 mm diameter samples of KRS-5 fibers; however, problems

were encountered in coupling into the HE_{11} mode with this high dielectric constant material. Waves were observed to propagate at 94 GHz on the 0.5 mm fibers, but they were evidently not in the HE_{11} mode, since they exhibited phase velocities only a few percent lower than the free-space velocity. One puzzling feature of these observations is that the waves appear to be substantially more closely confined to the surface of the fiber than theory would predict for higher order modes, and the bending losses appear to be much lower--0.2 meter radii 90 degree bends introduced at most a 1.5 dB loss transmission of a short section. This is the same sort of behavior observed in the earliest Hughes measurements. Measured attenuations were 20 to 24 dB/meter, much lower than the 860 dB/meter calculated for the HE_{11} mode using our measured values of loss tangent.

4. Scale-model studies with samples of KRS-5 and artificial dielectric materials ($\varepsilon' = 5, 10, 20$) were begun at 10 GHz in order to develop a better coupling scheme; a coupling technique using an intermediate dielectric constant material (e.g., $\varepsilon' = 10$) resulted from these studies, and it was used to excite the HE_{11} mode on the KRS-5 sample. Measurements of dielectric constant and loss tangent at 10 GHz deduced from the properties of the HE_{11} mode are in good agreement with our metallic waveguide measurements.

5. Additional information on the thallium halides was found in the literature, and from it a theoretical estimate of the behavior of loss tangent with frequency was made. The results are in good agreement with our 94 GHz measurements of bulk samples. This information is also contained in the paper mentioned in 1. above.

6. A computer program was written to make mode calculations in two-region fibers, and several combinations of core and cladding material were investigated. Using this program with the experimental results of the

bulk measurements, we are able to determine that a closely-confined fiber of KRS-5 with a thin clad of Teflon does not appear to be a practical transmission medium; however, a loosely-confined fiber with a thinner core of KRS-5 surrounded by approximately 5 cm diameter of foamed Teflon should exhibit a loss comparable to that of copper waveguide at 94 GHz, and have no more than double that loss with bends as small as 0.6 meter radius.

7. The theory of cylindrical dielectric waveguides with more than two regions was investigated, and a simple (but approximate) rule was developed for the relationships among the dielectric constants of the layers that would result in confining or radiating structures. Recent experiments by Yamamoto (Ref. I-4) measuring the losses in a gas-filled thin polyethylene tube as a millimeter-wave waveguide are in agreement with the predictions of this rule. The rule and the favorable results of the gas-filled guide suggest that a waveguide consisting of a core of flexible teflon foam with a thin layer of high dielectric constant material, for example, an overwrapped layer of thin KRS-5 fibers, could serve as a low-loss flexible transmission medium.

8. The state of the theory of dielectric waveguides with cross-sections of arbitrary shape and dielectric distribution was assessed. From this study we undertook the investigation of a technique based on the method of finite differences to calculate the propagation constants and field distributions in arbitrary waveguides.

C. Conclusions and Future Plans

It appears from our bulk measurements that there is little hope for a closely-confined thin fiber of KRS-5 surrounded by a thin layer of Teflon as a practical HE_{11} transmission medium; the bulk dielectric loss is simply too high. Moreover, the good agreement of the bulk loss

measurements with a simple but credible theory for losses in the thallium halides offers little hope that improvements in material purity, for example, can make a significant reduction in loss tangent. We do plan to measure directly the attenuation of the HE_{11} mode in a 0.5 mm KRS-5 fiber, now that we have a technique of coupling to it, to verify the calculations based on the bulk material measurements. We also plan to study the bending losses in smaller diameter, loosely-confined KRS-5 fibers, to see if our calculations for a practical flexible waveguide using these fibers are correct.

In addition, we are still faced with the puzzling result that we have observed, the propagation of a relatively low-loss mode (about 20 dB/meter) in a 0.5 mm fiber with a guide wavelength nearly that of free space (which would imply that almost all of the power resides outside the fiber), but which seems to have low bending losses. We hope to identify this mode and obtain quantitative agreement with theory.

We will also continue with the development of numerical techniques for determining the modes in dielectric waveguides of arbitrary cross section. We plan to apply this method to practical examples, particularly the rectangular dielectric waveguide with a large difference in dielectric constant between core and cladding. We feel that it is particularly important to obtain exact results for this configuration, since it is often used in rigid millimeter wave circuits with silicon or GaAs. Unfortunately, most workers seem to use the results derived by Marcatili (Ref. I-5) for small dielectric constant difference without concern for possible errors introduced by this violation of Marcatili's ground rules.

During the second year of this program we will begin the studies of evanescent-wave-coupled devices along the lines of those described in our proposal. We will begin with a study of the coupling from an ordinary

fiber to a fiber section made from an electro-optic or nonlinear material. We will also try to extend this study to artificial media, for example, an array of diodes with small antennas attached.

An additional area we wish to explore, one not originally described explicitly in the proposal, is a novel coupling configuration for the fiber-to-waveguide transition which employs a Fabry-Perot resonator. Under another program, we are studying the properties of an open Fabry-Perot cavity in which one mirror has a diffraction grating ruled on it. (Such a cavity is used in conjunction with an electron beam to generate millimeter waves; the Russian literature refers to such devices as "Diffraction Radiation Generators" (Ref. I-6).) We wish to see if this cavity structure can also be used to couple to the evanescent waves on a fiber. Since the coupling from standard metal waveguide to the cavity can be accomplished with a simple aperture, this may offer a superior (but probably narrow-band) method of coupling to fibers in the millimeter-wave range. However, it may also provide the means to couple to short lengths of non-linear or electro-optic materials in the form of fibers, to provide a reflection-type modulator or harmonic generator. Under another program we have already completed an analysis for the fields near the grating in an empty resonator, so that determining the coupling to a dielectric waveguide should not require much additional work.

D. Organization of this Report

The major areas of research summarized above are treated in more detail in the remainder of this report. The bulk measurements are described in Section II, in the form of a preprint of a paper prepared for submission to the IEEE Transactions on Microwave Theory and Techniques. Section III describes the dielectric waveguide measurements made to date. Section IV

reviews the theory of dielectric waveguides and presents our calculated losses for sample designs. It also discusses briefly the extension of the theory to waveguides of arbitrary cross-section and dielectric constant distribution. Finally, Section V presents the derivation and discussion of a simple approximate rule for predicting the general radiation loss behavior of multilayer cylindrical waveguides.

REFERENCES FOR SECTION I

I-1. D. A. Pinnow, A. L. Gentile, A. G. Standlee, and A. J. Timber, "Polycrystalline Fiber Optical Waveguides for Infrared Transmission," Appl. Phys. Lett., vol. 33, pp. 26-29 (1978).

I-2. A. E. Popa and R. E. Johnson, Hughes Research Laboratories, Malibu, CA; Unpublished Data, 1978.

I-3. W. B. Bridges, M. B. Klein, and E. Schweig, "Measurement of the Dielectric Constant and Loss Tangent of Thallium Mixed Halide Crystals KRS-5 and KRS-6 at 94 GHz," to be submitted for publication.

I-4. K. Yamamoto, "A Novel Low Loss Dielectric Waveguide for Millimeter and Sub-millimeter Wavelength," IEEE Trans. MTT, vol. MTT-28, pp. 580-584, (June 1980).

I-5. E. A. J. Marcatili, "Dielectric Rectangular Waveguide and Directional Coupler for Integrated Optics," BSTJ, vol. 48, pp. 2071-2102 (Sept. 1969).

I-6. V. P. Shestopalov, Diffraction Electronics, Translation of Difraktsionnaya Elektronika, Khar'kov Press 1976; Translated by U. S. Joint Publication Service, April 1978.

II. BULK DIELECTRIC MEASUREMENTS

The following paper has been prepared for submission to the IEEE Transaction on Microwave Theory on Techniques.

MEASUREMENT OF THE DIELECTRIC CONSTANT AND LOSS TANGENT OF THALLIUM MIXED HALIDE CRYSTALS KRS-5 AND KRS-6 at 94 GHz(*)

by

William B. Bridges(a), Marvin B. Klein(b), and Edgard Schweig(a)

ABSTRACT

The dielectric constants and loss tangents of KRS-5 and KRS-6 thallium halide mixed crystals have been measured at 94 GHz using both the shorted waveguide reflection method and the Fabry-Perot transmission method on samples filling standard WR-10 waveguide. The results—KRS-5: $\varepsilon_r' = 31.2 \pm 0.7$, $\tan\delta = 1.8 \pm 0.2 \times 10^{-2}$; KRS-6: $\varepsilon_r' = 29 \pm 1$, $\tan\delta = 2 \pm 1 \times 10^{-2}$—agree reasonably well with a simple theoretical fit to the far-infrared lattice absorptions of TlBr and TlCl at about 1400 GHz. The dielectric samples were hot-pressed into copper wafers with dimensions matching WR-10 waveguide, and then machined and polished to obtain flat, parallel air-dielectric interfaces.

(*) Work sponsored by the Office of Naval Research under contract number N00014-79-C-0839 and by Hughes Aircraft Co. Independent Research and Development Funds.

(a) California Institute of Technology, Department of Electrical Engineering, Pasadema, California 91125

(b) Hughes Research Laboratories, Malibu, California 90265.

Introduction

The mixed crystal thallium bromide-iodide (KRS-5) has long been known as an infrared transmitting window material for the wavelength range 0.6 to 40 microns. However, little was known about its microwave transmission properties, and nothing of its properties in the millimeter wave range. Recently, long fibers of KRS-5 have been fabricated, and their infrared transmission has been reported[1]. Soon afterward propagation in a KRS-5 fiber at 94 GHz was demonstrated[2], thus raising the possibility of waveguide applications in the millimeter wave range. The low frequency dielectric constant of KRS-5 is given by von Hippel[3] as 32, which would imply a very small fiber diameter for such a mm-wave guide (less than 1 mm diameter) and allow a wide range of dielectrics for cladding material, for example, Teflon or polyethylene. Von Hippel also reports a loss tangent of 2×10^{-3} in KRS-5 at 10 GHz[3], while Popa and Johnson[2] measured a value of 2.3×10^{-3} at 37 GHz. The losses are expected to be larger at higher frequencies due to lattice absorption, but no literature values are available. The reported low-frequency losses in KRS-6 (thalium bromide-chloride) are also quite low[3]. Accordingly, we undertook a study of the dielectric properties of KRS-5 and KRS-6 at 94 GHz to assess the potential of these materials in a practical flexible waveguide.

Our measurement techniques utilize samples mounted in standard metal waveguide, in contrast to past work at 94 GHz, which was based primarily on quasi-optical techniques. Our preference arises from the simplicity and accuracy of waveguide techniques and a novel sample mounting configuration which eliminates gaps between sample and wall. Two different waveguide measurement techniques were used with the same samples:

1. Measurement of the transmission through or reflection from a planar slab of dielectric, taking into account the multiple reflections between the two faces—a Fabry-Perot resonator. (Our method is a modification of that described by Redheffer[5];)

2. Measurement of the reflection from a sample backed by a short (a well-known technique; cf. Roberts and von Hippel[4].)

In addition, samples of Teflon and Rexolite were measured by these same two techniques as a check on the validity and accuracy of the methods.

Sample Preparation

In preparing samples for any waveguide measurement, it is very important that a tight fit be obtained to the waveguide walls. The errors introduced by any gap between the wall and the sample increase as the dimensions of the waveguide and sample decrease and as the dielectric constant increases. In order to obtain the best fit for the 94 GHz measurements, the samples of KRS-5 were hot-pressed into a waveguide-shaped opening in a copper wafer. The cross section of the opening was 2.54 x 1.27 mm, corresponding to standard WR-10 waveguide. This opening was formed by electroplating a thick layer of copper onto a precision machined aluminum mandrel, and then etching away the mandrel. Before the copper electroplating, a thin (5 μm) layer of gold was evaporated on the mandrel; after electroplating and etching, this gold layer remains on the interior surfaces of the waveguide and prevents oxidation during the hot pressing procedure.

Samples of KRS-5 and KRS-6 were machined from commercial stock* into billets which were slightly undersize in both thickness and transverse dimensions. A sample was then inserted into a wafer opening and pressed with an undersized mandrel.

*The sources of the materials were: KRS-5, Harshaw Chemical Co., Solon, Ohio; KRS-6, British Drug House, Poole, England.

at an elevated temperature until it expanded laterally to fill the opening. The best results were obtained by applying $\sim 2 \times 10^6$ kg/m^2 for periods of six hours at a temperature of 250°C. The wafers with the sample in place were then machined to the desired thickness and lapped to obtain a flat, polished surface.

The KRS-5 samples prepared in this manner were free from cracks or voids under inspection by microscope. Typical samples are shown in Fig. 1. KRS-6 is substantially less ductile than KRS-5, and the pressed samples of this material were not as free from defects. Waveguide wafers containing samples of Teflon and Rexolite were also prepared by hot pressing. Because of the high ductility of Teflon, lower values of pressure and temperature were used when pressing the material.

Waveguide Fabry-Perot Measurements

The first measurement technique used the wafers as Fabry-Perot resonators in a waveguide; different combinations of samples are inserted to vary the length of the resonator. The arrangement shown in Fig. 2a was employed to measure the transmission and reflection from the dielectric wafers. A waveguide isolator was used to prevent frequency pulling of the klystron source by reflections from the samples; a second isolator was used in front of the transmission detector to eliminate reflections from any detector mismatch. A reference transmission level was first established with no wafers in the system. Transmission and reflection coefficients with the wafers in place were then determined by changing the precision attenuator until the detector signals were equal to the reference level, thus eliminating detector non-linearity as a source of error.

The power transmission coefficient at normal incidence through a plane-parallel dielectric sample filling the waveguide cross section is given by

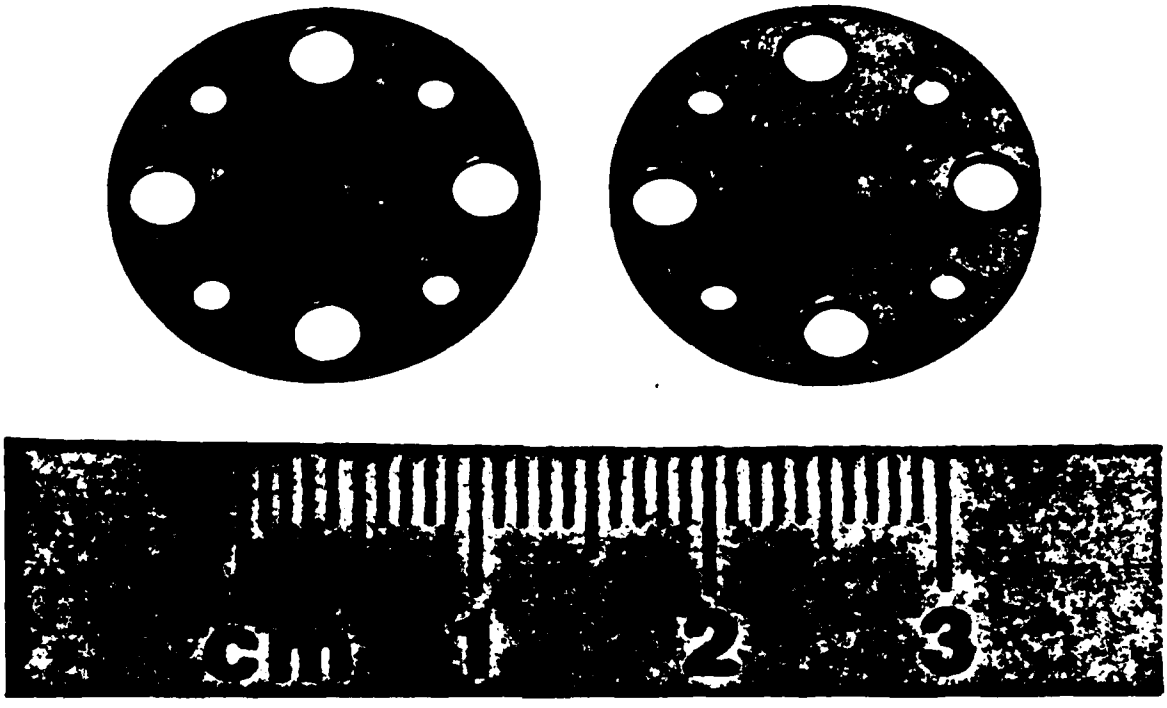

Figure 1 Photograph of the copper-wafer-mounted samples of KRS-5.

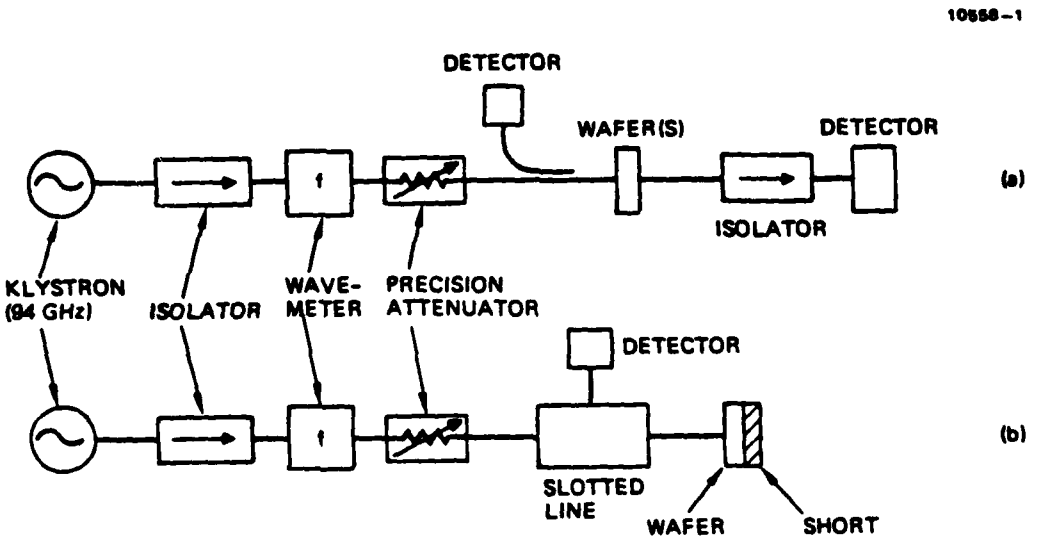

Figure II-2 Experimental arrangements used for the waveguide measurement of complex dielectric constant.

(a) Fabry-Perot resonances in reflection and transmission;

(b) Shorted-waveguide method.

$$\frac{P_{transmitted}}{P_{incident}} = \frac{1}{\frac{[1 - R\exp(-2\alpha L)]^2}{(1 - R^2\exp(-2\alpha L)} + \frac{4R}{(1 - R)^2}\sin^2\beta L} \quad (1)$$

where R is the power reflection coefficient of a single air-dielectric interface and $\alpha + j\beta$ is the complex propagation constant for TE_{10} waves in the dielectric-filled region:

$$\alpha = \frac{\pi}{\lambda} \cdot \frac{\varepsilon_r''}{\sqrt{\varepsilon_r' - \left(\frac{\lambda}{2a}\right)^2}} = \frac{\pi}{\lambda} \tan\delta \frac{\varepsilon_r'}{\sqrt{\varepsilon_r' - \left(\frac{\lambda}{2a}\right)^2}} \quad (2)$$

$$\beta = \frac{2\pi}{\lambda}\sqrt{\varepsilon_r' - \left(\frac{\lambda}{2a}\right)^2} \quad (3)$$

where λ is the free space wavelength, a is the width of the waveguide, $\varepsilon_r' - j\varepsilon_r''$ is the complex relative dielectric constant, and $\tan\delta$ is the loss tangent. These expressions are valid for low-loss materials ($\tan\delta << 1$). Further, for the situation of a high dielectric constant material filling a TE_{10} waveguide operated above its normal (air-filled) cutoff frequency, the factor $(\lambda/2a)^2 << \varepsilon_r'$, so that the approximations

$$\alpha = \frac{\pi\sqrt{\varepsilon_r'}}{\lambda} \tan\delta \quad (2a)$$

$$\beta = \frac{2\pi\sqrt{\varepsilon_r'}}{\lambda} \quad (3a)$$

are valid.

The reflection coefficient R in Eq. 1 is simply the Fresnel reflection from an air-dielectric interface, modified by the change in phase velocity resulting from the presence of the metallic waveguide walls:

$$R = \left[\frac{\sqrt{\varepsilon_r' - \left(\frac{\lambda}{2a}\right)^2} - \sqrt{1 - \left(\frac{\lambda}{2a}\right)^2}}{\sqrt{\varepsilon_r' - \left(\frac{\lambda}{2a}\right)^2} + \sqrt{1 - \left(\frac{\lambda}{2a}\right)^2}} \right]^2 \qquad (4)$$

As before, if $(\lambda/2a)^2 << \varepsilon_r'$, then

$$R \approx \left[\frac{\sqrt{\varepsilon_r'} - \sqrt{1 - \left(\frac{\lambda}{2a}\right)^2}}{\sqrt{\varepsilon_r'} + \sqrt{1 - \left(\frac{\lambda}{2a}\right)^2}} \right]^2 \qquad (4a)$$

For $\varepsilon_r' = 32$ and $\lambda = 3.0$ mm, $R \approx 0.76$ in a WR-10 waveguide.

Equations 1-4 assume, of course, that all the power remains in the TE_{10} mode as the wave passes through the dielectric-filled section, despite the fact that many higher-order modes are above cut-off in that section. We argue for this simplification by noting that the planar, normal air-dielectric interfaces and the constant physical cross section of the metallic boundaries do not encourage mode conversion. Nevertheless, this could be a source of error in long sample sections.

The transmission and reflection for all possible combinations of wafer thicknesses were measured at a fixed frequency of 94.75 GHz. These data were then used as input to a computer program that systematically varied the complex dielectric constant to yield a least-squared-error fit of the theoretical transmission or reflection coefficient to the data. Several sets of measurements were made with the KRS-5 and KRS-6 wafers under different conditions as specified in Table I. Figure 3 shows the data points corresponding to a specific run for KRS-5 and illustrates the quality of the fit to the theoretical transmission (solid curve). The reduced accuracy for the KRS-6 measurement is presumed to be due to sample imperfections, which had an expecially strong effect when several samples were stacked together to give large thicknesses.

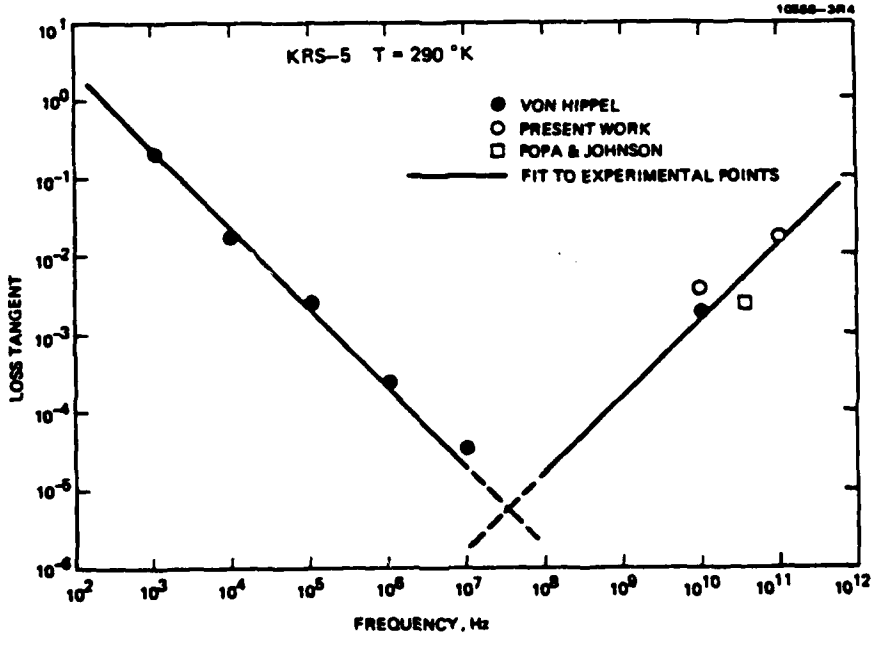

Figure II-3 Measured transmission coefficients and fitted Fabry-Perot curve for KRS-6 wafer samples.

In order to check on the accuracy of this technique and its ability to measure still lower values of loss tangent, we also measured the dielectric constant and loss tangent of Rexolite and Teflon. The measured values are were:

$\varepsilon_r' = 2.56$, $\tan\delta = 3 \times 10^{-3}$ for Rexolite,

$\varepsilon_r' = 2.04$, $\tan\delta = 9 \times 10^{-3}$ for Teflon.

The values of dielectric constant are in good agreement with literature values[6,7], while the values of loss tangent are larger by a factor of ~ 3 (for Rexolite) and ~ 10 (for Teflon). We do not know if this discrepancy is due to measurement error or sample imperfections. In any case the measured values of loss tangent for these materials are lower than the values for KRS-5 and KRS-6, and suggest that the technique should be accurate for the latter materials.

From our experience, it appears that in the case of high-dielectric constant material, the best data are obtained from the measurement of the transmission coefficient, whereas for low-dielectric constant material the reflection coefficient should be used, and a fit made to the reflection equation analogous to Eq. 1:

$$\frac{P_{reflected}}{P_{incident}} = \frac{\dfrac{R[1 - \exp(-2\alpha L)]^2}{(1 - R)^2 \exp(-2\alpha L)} + \dfrac{4R}{(1 - R)^2}\sin^2\beta L}{\dfrac{[1 - R\exp(-2\alpha L)]^2}{(1 - R)^2 \exp(-2\alpha L)} + \dfrac{4R}{(1 - R)^2}\sin^2\beta L} \qquad (6)$$

For Teflon and Rexolite it is not appropriate to use the high dielectric constant approximations 2a–4a; the exact expressions 2–4 are used instead.

Waveguide Reflection Measurements

In a second experiment we measured the complex reflection coefficient from a single wafer inserted at the shorted end of a waveguide. An experimental arrangement similar to the one described by Roberts and von Hippel[4] was used for the reflection measurements, as shown in Fig. 2b.

A short was placed at the end of the empty waveguide, creating a reference standing wave pattern. The position of a node was determined with a slotted line (TRG Model W740). A wafer was then inserted between the end of the waveguide and the short, and the position and magnitude of the standing wave were again determined with the slotted line. As before, the precision attenuator was used to return the detector output to the reference level, so that the VSWR accuracy depended solely on the attenuator calibration, and not on the detector linearity. The measurements were made at a frequency of 94.75 GHz.

The theoretical equation relating the shift to the VSWR minimum from the reference position and VSWR magnitude to the complex dielectric constant of the sample is transcendental and implicit in dielectric constant:

$$\frac{\tanh[(\alpha + j\beta)L]}{[(\alpha + j\beta)L]} = -\frac{j\lambda_g}{2\pi L} \frac{\text{VSWR}^{-1} - j \tan\left(\frac{2\pi S}{\lambda_g}\right)}{1 - j\,\text{VSWR}^{-1} \tan\left(\frac{2\pi S}{\lambda_g}\right)} \qquad (7)$$

where λ_g is the wavelength in the air-filled guide and S is the distance from the dielectric interface to the first node of the standing wave in the air-filled sections; S is also equal to the shift in position of the standing wave mode when the sample is inserted. As before, the assumption is that the power remains in the TE_{10} mode throughout, even though higher-order modes can exist in the dielectric-filled section.

The right hand side of 7 contains the measured quantities and is evaluated, resulting in a single complex number. The propagation constant $\alpha + j\beta$ is then determined numerically from this complex number and $\varepsilon_r' - j\varepsilon_r''$ from $\alpha + j\beta$ by Eqs. 2 and 3. A computer program to solve these equations was written along the lines of the program used by S. Nelson, et al.[9].

The values of complex dielectric constant obtained for the samples of KRS-5 and KRS-6 are given in Table II. The agreement between the various samples is quite good and provides an increased level of confidence in the results.

In order to provide a further check on our experiments, we measured the dielectric properties of Rexolite and Teflon at 94 GHz and obtained a good agreement with values published in the literature[6,7]. Unfortunately, the wafer-mounted samples of Teflon and Rexolite were not thick enough to yield good results. In the case of very low-loss, low dielectric constant materials, it is necessary to use samples that are significantly larger physically because the additional losses when the dielectric is introduced in the waveguide must be larger than the losses due to the metallic walls. Accordingly, we cut longer samples of Teflon and Rexolite ($\sim$ 13 mm) for a slip fit in WR-10 waveguide from the same lots of Teflon and Rexolite used for the wafers. Our results with these samples were:

$\varepsilon_r' = 2.4 \pm 0.1$, $\tan\delta = (3.3 \pm 0.1) \times 10^{-3}$ for Rexolite and

$\varepsilon_r' = 1.9 \pm 0.1$, $\tan\delta = (3.9 \pm 0.9) \times 10^{-3}$ for Teflon.

As a check on the 10 GHz values of ε_r' and $\tan\delta$ quoted without reference by von Hippel[3] for KRS-5, we also made a waveguide reflection measurement at 10 GHz, using a setup similar to the one depicted on Fig. 2b. In this

case, the samples were machined to size and slipped into the end of standard X-band waveguide. The average values for the complex dielectric constant of KRS-5 at 10 GHz were:

$$\varepsilon' = 30.6 \pm 0.8, \tan \delta = (4 \pm 2) \times 10^{-3}.$$

Frequency Dependence of Dielectric Properties

As stated earlier, no measurements of the dielectric properties of KRS-5 or KRS-6 above 10 GHz have been reported previously. However, measured values are available at lower frequencies, especially for KRS-5. Our measured values of ε_r' at 10 and 94 GHz for KRS-5 are essentially the same as the values reported by von Hippel[3] at 10^2 - 10^7 Hz and 10^{10} Hz. In order to compare our measured values of loss tangent for KRS-5 with the other values, we have plotted all measurements as a function of frequency in Fig. 4. It is clear that the frequency variation can be divided into two separate regimes. Below $\sim 10^8$ Hz ionic conductivity dominates and the loss tangent varies as

$$\tan \delta = \frac{1}{2\pi f \rho \varepsilon_r' \varepsilon_o} \tag{8}$$

where f is the frequency and ρ is the resistivity. As expected, the data points closely follow a 1/f variation, corresponding to $\rho = 2 \times 10^8$ ohm-cm and $\varepsilon_r = 31$. The absorption at microwave and millimeter wavelengths appears to be dominated by the low frequency tail of the strong lattice absorption centered at $\sim$ 1400 GHz. If we model the lattice vibration as a single harmonic oscillator, the loss tangent is expected to vary as

$$\tan \delta = \frac{\gamma f}{2\pi f_o^2} \tag{9}$$

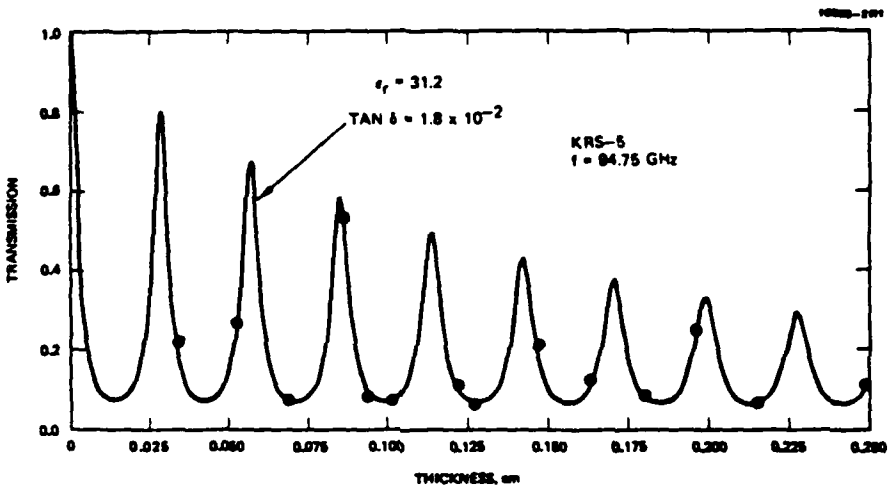

Figure II-4 Measured values of the loss tangent of KRS-5 and theoretical behavior due to ionic conductivity (10^3 to 10^7) Hz and lattice absorption (above 10^7 Hz). Curves for the theoretical variation of loss tangent of TlCl and TlBr due to simple lattice vibrations are also shown.

where γ is the damping coefficient (rad^{-1}) and f_o is the resonant frequency. In Fig. 3 we have drawn a line through the data points that gives a value of $\gamma/2\pi f_o^2 = 1.5 \times 10^{-13}$ sec. Separate measured values of γ and f_o for KRS-5 are unavailable, but literature values[10] for TlCl and TlBr (based on dielectric constant measurements in the far infrared) give $\gamma/2\pi f_o^2 = 1.2 \times 10^{-13}$ and 1.1×10^{-13} sec, respectively. No value is available for TlI, but we would expect it to be similar, and thus the admixture of TlI to TlBr (giving KRS-5) is also expected to be comparable. It appears that our measured value for KRS-5 may be slightly high due to extrinsic factors such as impurities and imperfections.

Summary

In summary, we have provided the first measured value of the dielectric properties of KRS-5 and KRS-6 at 94 GHz. Our measurement techniques made use of sample mounting in standard metal waveguide, thus reducing the required sample size and eliminating the diffraction problems present in quasi-optical techniques. Our sample mounting technique insures a perfect fit into the waveguide, and is applicable to a wide range of ductile materials. We are now working to extend the technique to harder materials.

We would like to acknowledge helpful discussions with A. E. Popa and D. M. Henderson, as well as the expert technical assistance of R. E. Johnson.

TABLE I

Experimental Values of ϵ_r' and Tan δ by the Waveguide Fabry-Perot Method at 94.75 GHz

Run	Material	ϵ_r'	Tan δ	Method[a]	Fit[b]	Wafer Thicknesses (mm)	Comment
1	KRS-5	31.2	1.8×10^{-2}	T	0.01	0.335, 0.526, 0.686, 0.940	
2	KRS-5	30.5	2×10^{-2}	T	0.075	0.315, 0.516, 0.678, 0.932	wafers of run #1 machined and repolished
3	KRS-5	30.4	1.9×10^{-2}	T	0.019	Same as run 2, plus 0.414, 0.947	only combinations up to 3 wafers at a time taken
4	KRS-6	28.5	2.3×10^{-2}	T	0.11	0.310, 0.358, 0.483, 0.777, 0.973	
5	KRS-6	28.9	2.3×10^{-2}	T	0.11	0.307, 0.357, 0.483, 0.775, 0.968	wafers of run #4 repolished
6	KRS-6	25.5	1.4×10^{-2}	T	0.0014	0.307, 0.357, 0.483	only thinnest 3 wafers of run #5 used
7	Teflon	2.04	9×10^{-3}	R	0.0029	0.818, 1.288, 1.849	
8	Rexolite	2.56	2.6×10^{-3}	R	0.0061	0.812, 1.285, 1.88	

Notes: (a) T = transmission, R = reflection measured to fit to theory

(b) Root mean square deviation of data points from theory.

TABLE II

Experimental Values of ε_r' and Tan δ by the Shorted Waveguide Method

Sample Thickness (mm)	Material	ε_r'	Tan δ
0.942	KRS-5	31.7	1.7×10^{-2}
0.940	KRS-5	31.9	1.7×10^{-2}
0.686	KRS-5	31.1	1.9×10^{-2}
0.414	KRS-5	31.5	1.6×10^{-2}
0.973	KRS-6	30.8	1.1×10^{-2}
0.777	KRS-6	31.0	3.3×10^{-2}
0.483	KRS-6	30.8	3.6×10^{-2}
0.358	KRS-6	30.8	1.0×10^{-2}
12.532	Rexolite	2.41	3.4×10^{-3}
12.517	Rexolite	2.41	3.2×10^{-3}
14.030	Teflon	1.94	4.1×10^{-3}
13.872	Teflon	1.98	4.7×10^{-3}

References

1. D. A. Pinnow, A. L. Gentile, A. G. Standlee, and A. J. Timber, "Polycrystalline Fiber Optical Waveguides for Infrared Transmission," Appl. Phys. Lett., 33, pp. 26-29 (1978).

2. A. E. Popa and R. E. Johnson, Hughes Research Laboratories, unpublished data, 1978.

3. A. von Hippel, Dielectric Materials and Applications, John Wiley & Sons, Inc., New York 1954, pp. 302, 274, 375.

4. S. Roberts and A. von Hippel, "A New Method for Measuring Dielectric Constant and Loss in the Range of Centimeter Waves," J. Appl. Phys., 17, pp. 610-616 (1946).

5. R. M. Redheffer, "The Measurement of Dielectric Constants," in Technique of Microwave Measurements, C. G. Montgomery, Ed., McGraw-Hill, New York 1947, Ch. 10.

6. K. H. Breeden and A. P. Sheppard, "A Note on the Millimeter and Submillimeter Wave Dielectric Constant and Low Tangent Value of Some Common Materials," Radio Science, Vol. 3 (new series), no. 2, pp. 205 (Feb. 1968).

7. F. Sobel, F. L. Wentworth and J. C. Wiltse, "Quasi-optical Surface Waveguide and Other Components for the 100 to 300 GHz Region," IRE Trans. MTT, pp. 512-518, (Nov. 1961).

8. A. von Hippel, Dielectric Materials and Applications, John Wiley & Sons, Inc., New York, pp. 67 (1954).

9. S. Nelson, C. Schlaphoff, L. Stetson, "Computer Program for Calculating Dielectric Properties of Low or High-Loss Materials from Short-Circuited Waveguide Measurements," U.S. Dept. of Agr. Report # ARS-NC-4 (Nov. 1972).

10. A. P. Lowndes and D. H. Martin, "Dielectric Dispersion and the Structure of Ionic Lattices," Proc. Roy. Soc. A.308, pp. 474-496 (1969).

III. DIELECTRIC WAVEGUIDE EXPERIMENTS (W. B. Bridges, M. B. Klein, E. Schweig)

Some of the experimental results we have obtained with dielectric waveguides are still a bit puzzling; for this reason, our experiments will be described in chronological order, so that the reader will have the benefit of following our reasoning as well as our results. We hope that by the time of the next annual report, the puzzles will be solved and experiment and theory will again be in good agreement.

A. Original Hughes Measurements

The first measurements at 94 GHz on KRS-5 fibers were made by Popa and Johnson at Hughes Research Laboratories in 1978 (Ref. III-1). The measurements were largely qualitative, and new job assignments precluded a quantitative follow-up. The gist of their results are as follows: A KRS-5 fiber 0.5 mm in diameter and about 2 meters long was coupled to a klystron signal source at one end and a Schottky detector at the other. The coupling sections were the same as those described in the next section, a Rexolite bicone in the end of a flared waveguide. Transmission was observed through this length of fiber, but the attenuation was not measured. The magnitude of the transmitted signal did not seem to depend significantly on the bending or looping of the 2 meter length of fiber. The guide wavelength on the fiber was observed to be about 5% less than the free space wavelength as determined by measuring the periodicity of the reflected power as a small metal perturber was slid along the fiber. The fields also appeared to hug the fiber very closely; all of the power could be transmitted when the fiber was threaded through a 1/4 inch hole in a metal plate.

All of these same observations have been repeated by us on a somewhat shorter length of fiber (50 cm), as reported in more detail below.

However, it is interesting to note first two facts about the Popa-Johnson measurements:

1. The observation of a guide wavelength near that of the free space wavelength should have raised an eyebrow at the time it was seen; but Popa and Johnson had previously made a filled, slotted waveguide measurement of KRS-5 at 35 GHz, and had concluded that the dielectric constant was 19, not 32 (a mistake that resulted from misreading the rather complex standing wave pattern on their slotted section.) For a fiber diameter of 0.5 mm and $\varepsilon' = 19$, one would expect only the HE_{11} mode to propagate and that it would have a guide wavelength nearly that of free space.

2. If our bulk measurement value of the loss tangent of KRS-5 is used to predict the transmission loss of an HE_{11} mode on a 0.5 mm diameter fiber with $\varepsilon' = 32$, the loss would be about exp (-400), or about -1730 dB. Obviously, Popa and Johnson were not seeing the HE_{11} mode in their experiment. It is also clear that they were not seeing simple radiation from the source coupler to the detector coupler directly through space--the transmission occurred via a guided mode closely hugging the guide, and could be cut off completely by closing down a metal iris anywhere along the guide. It was on the basis of these experiments that we decided to investigate further and wrote the proposal that lead to the present program.

B. Initial 94 GHz Measurements Under the Present Program

As our initial experiment we attempted to duplicate the results obtained by Popa and Johnson. The experimental arrangement is shown in Fig. III-1. The same couplers were used to excite the fiber as those used by Popa and Johnson; they are shown in Fig. III-2. A biconical Rexolite bead with a hole slightly larger than the fiber is inserted into the flared

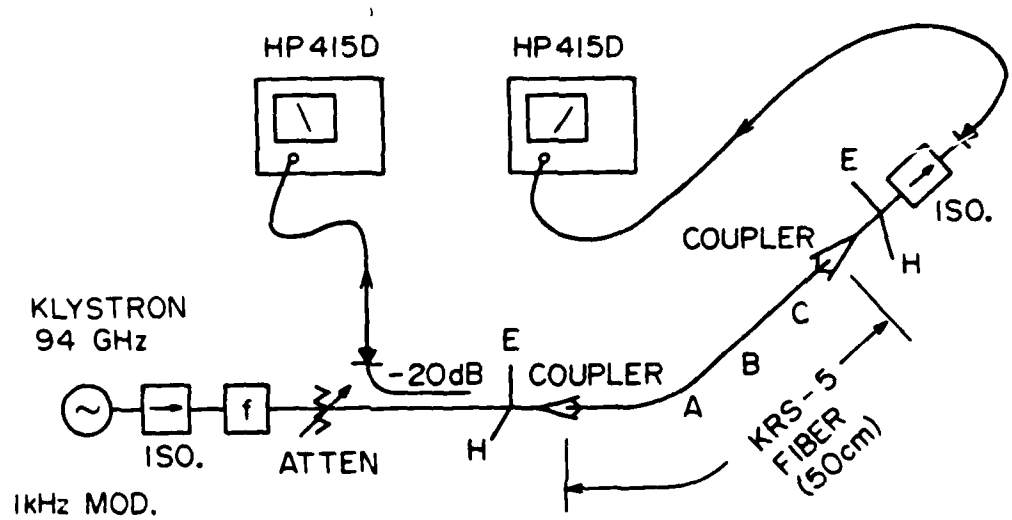

Figure III-1 Experimental arrangement used at 94 GHz to study the propagation along KRS-5 and KRS-6 fibers. A small metal perturber was slid along the outside of the fiber at positions A, B, and C to determine the change in reflected power due to the fiber propagation loss.

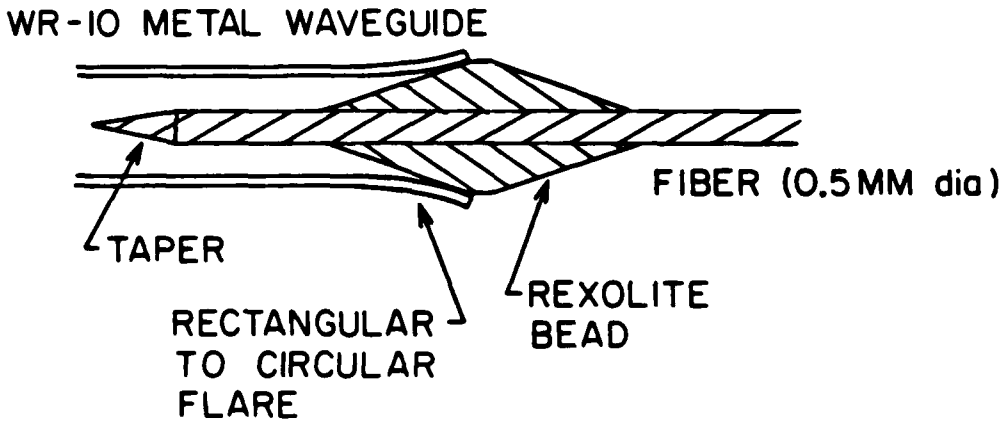

Figure III-2 Cross-section of the couplers used in the initial fiber experiments. The fiber can be slid through the bead to find an optimum coupling.

end of a standard WR-10 waveguide section. The flare also serves as a transition from the standard rectangular cross section to a round cross section that fits the bead. The tip of the KRS-5 fiber was carefully sanded to a conical taper with an approximately 3:1 aspect ratio, about the limit for hand sanding.

The fiber is inserted into the hole in the bead and the depth of penetration is adjusted for maximum transmission. The E-H tuners are then further adjusted for maximum transmission; the fiber penetration and E-H tuner settings appear to be independent. One precaution taken in adjusting the fiber penetration was to offset the receiving coupler from the line of sight of the transmitting coupler; if the fiber is not positioned properly (e.g., too shallow) then the transmitting coupler radiates like a horn antenna and the receiving coupler picks it up directly if the two are pointed at each other. Even if the couplers are offset in angle as shown in Fig. III-1, direct radiation could be reflected from one to the other by a flat metal plate used as a mirror. However, with proper penetration of the fiber into the waveguide, no free space radiation could be detected either by spurious transmission from mirror-like reflectors, or as changes in reflected power. With proper fiber positioning, the fields appeared to be localized within 1 mm around the fiber.

With the arrangement of Fig. III-1, we were able to reproduce all of the observations made by Popa and Johnson. By moving a small metal perturber (a slotted metal plate or a small wire ring) along the fiber with a calibrated stage (a Hewlett-Packard slotted line carriage), we measured a guide wavelength a few percent less than the free space wavelength to within our measurement accuracy (perhaps 5%) by observing the periodic variation in the reflected power. The fiber was also bent in a single curve from nearly

straight to 90 degrees with no more than 1.5 dB decrease in the transmitted signal level.

In addition to verifying the earlier qualitative observations, we also attempted to measure the guide attenuation directly. About 22 dB attenuation had to be added on the precision variable attenuator to return the detector output to the original value when the fiber section and couplers were removed. This loss in a 50 cm length gives a value of 0.45 dB/cm if all the loss is attributed to the fiber and none to the couplers. This value is certainly much less than the 8.6 dB/cm that we now calculate from our loss tangent measurements for a tightly-confined mode in a KRS-5 fiber. However, we had not yet made the loss tangent measurements, and we were surprised that the losses were as high as 0.45 dB/cm.

We then attempted another loss measurement by noting the change in the magnitude of the reflected power variation induced by the moving perturber as it is slid along different sections of the guide (A, B, and C in Fig. III-1). The reflected power variation when the perturber is moved along the fiber results from the interference of the reflection from the perturber with other reflections in the guide (most likely the coupler mismatch). The magnitude of the variation decreases as the perturber is moved to regions farther from the transmitter, since the wave reflected from the perturber is attenuated by the additional double pass loss in the length to these regions. From these measurements we concluded that the fiber attenuation was between 0.20 and 0.24 dB/cm, or 20 to 24 dB/meter for KRS-5 and about 12 dB/meter for KRS-6, and that the remaining attenuation we observed in the section was attributable to the couplers.

Once we began to obtain data from the bulk measurements of KRS-5, we realized that a dielectric constant of 32 and a diameter of 0.5 mm

should have produced a very significant slowing of the wave on the fiber (see Section IV for the theoretical curves for a 0.5 mm fiber of $\varepsilon' = 32$.) Even though the symmetry of the coupler design should have excited primarily the HE_{11} mode, we concluded that we were actually seeing some other mode. We probed near the fiber with a thin wire in an attempt to determine the polarization and distribution of the electric fields. This proved unsuccessful in that any orientation of the wire probe seemed to produce the same value of reflection. We also attempted to rotate the detector mount, slipping the fiber in the Rexolite bead to determine if the mode were plane polarized or not. This proved to be inconclusive, since it was very difficult to keep the fiber fixed and slip it in the bead repeatably.

From the loss tangent values we could conclude that if the HE_{11} mode were excited by the couplers, it would decay very rapidly near the transmitting coupler, and we would not see it at the positions A, B, or C where we had made the perturbations. We attempted to make the same kind of perturbation measurements near the transmitting coupler without success, since there was sufficient free space radiation in that vicinity to interfere and give a complicated pattern of reflections when the perturber was moved. With all these courses of action frustrated, we decided to set up a scale model measurement arrangement at X-band, where the physical dimensions are ten times larger, and where artificial dielectric materials in a variety of dielectric constants are available for experiments to improve the matching scheme.

C. Dielectric Waveguide Measurements at 10 GHz

An experimental arrangement to excite waves on dielectric rods was set up at 10 GHz as shown in Fig. III-3. Only short, rigid dielectric samples were available for this wavelength, so that transmission measurements, which require a bend in the fiber, were not attempted. A

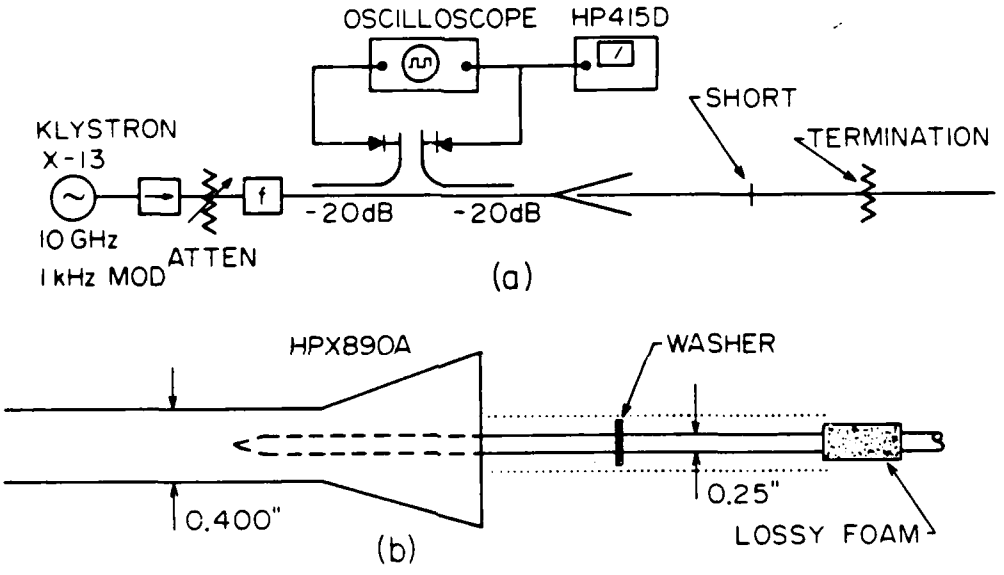

Figure III-3 (a) Experimental arrangement used at 10 GHz to study the HE_{11} propagation along dielectric rods.

(b) Detail of the rod and horn coupler used. The fields around the fiber were determined to extend only out to the dotted line as determined by observing the reflections from a metal perturber.

standard horn antenna with its flare in the direction of the electric field was used as a coupler to the waveguide. A polyfoam insert was fit to the inside of the horn to provide centering and support for the dielectric rods. Samples of Lucite, Stycast* artificial dielectric materials, and KRS-5 were studied with the results tabulated in Table III-1.

For Lucite and ($\varepsilon' = 10$ Stycase rods, good coupling to the HE_{11} mode was easily obtained by simply inserting the rod in the end of the horn as shown in Fig. III-3b. (A blunt taper was ground on the end of each rod, but the coupling to the HE_{11} mode appeared to be as good with or without the taper; the reflection coefficient was somewhat higher without the taper.) The rod was positioned in the horn to minimize the reflected power and minimize the radiation field away from the dielectric rod. For Lucite and $\varepsilon' = 10$ Stycast it was possible to eliminate the radiation field completely; a metal perturber could be placed anywhere outside the volume occupied by the HE_{11} mode (indicated schematically by the dotted line surrounding the rod in Fig. III-3b) with no change in reflected power.

As another test of the degree of coupling to the HE_{11} mode, the rod was removed and a shorting metal plate was placed over the end of the horn to establish a 100% reflected power reference reading. The rod was then replaced and standard 1/4 inch washer was slipped over the rod as shown in Fig. III-3b. Essentially 100% reflected power could also be obtained from this washer, which was only about 5/8 inch in diameter, indicating that the fields of the mode excited extended only about one rod diameter or less outside the rod.

---

* A trade name for materials from Emerson & Cumings, Canton, MA.

By moving the washer along the rod and observing the periodic change in the reflected power reading, the guide wavelengths were determined; these are compared with theory in Table III-1. (No theoretical value is given for the square sample since the theory for this geometry is not known; however, the result is consistent with a simple approximation that takes an "effective diameter" as the diagonal dimension of the square.) The agreement with the theoretical values for the HE_{11} mode is generally good.

As a further test for the existence of the HE_{11} mode, the fields surrounding the rod were probed with a short length of wire in the positions shown in Fig. III-4; the electric field lines for HE_{11} vertically polarized mode are also sketched in. With the wire probe in position A, very little change in reflected power was observed as the wire was moved along the rod. With the wire in position B, a very large change in reflected power was observed as the wire was moved. With the wire oriented in position C an intermediate value of reflection was observed, and with the wire in position D, the largest change in reflection was observed. These observations are all consistent with the degree to which the electric field of an HE_{11} mode would be shorted by the presence of the wire probe.

When the same sequence of measurements was attempted with the higher dielectric constant rods (Stycast $\varepsilon' = 20$, 30, and KRS-5) quite a different behavior was noted. First, simply inserting the rods into the end of the horn was insufficient to couple to the desired HE_{11} mode. The free space radiation from the end of the horn was so strong that it was impossible to measure the guide wavelength by sliding a shorting washer along the guide--the free space value was obtained no matter what the location of the perturber.

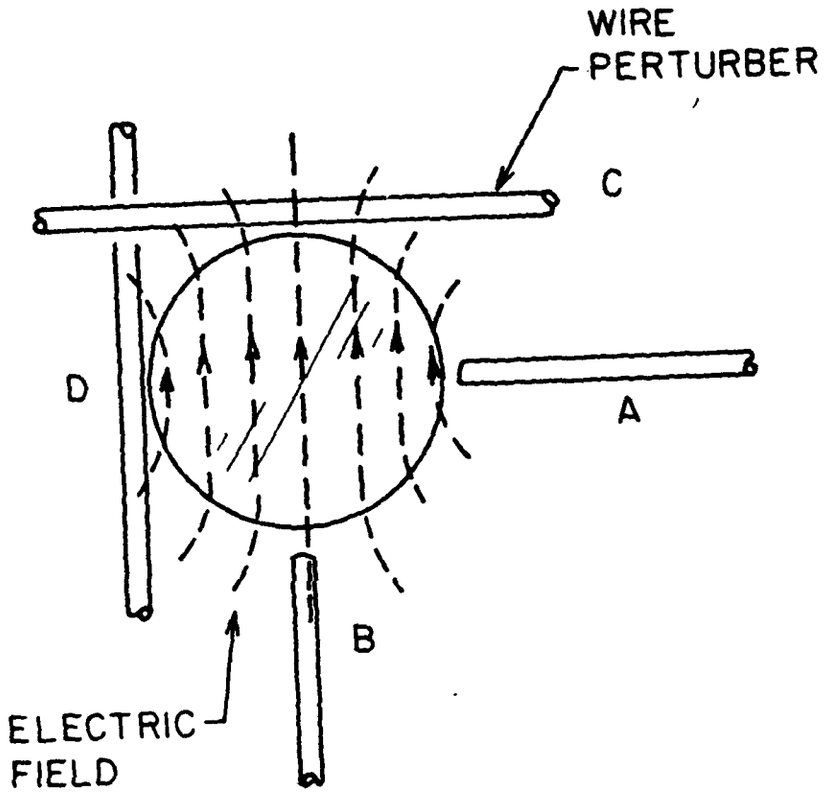

Figure III-4 Cross-section of the dielectric rod showing four positions of a metal wire perturber. The electric field lines are sketched in for the HE_{11} mode in a particular plane; beyond the plane shown the electric field lines run parallel to the rod along the outside, then turn back into the fiber one half guide wavelength away, reproducing the pattern shown, but in the opposite sense.

After some creative trial and error, the arrangement shown in Fig. III-5 was developed to excite a HE_{11} mode on the KRS-5 sample. The coupling was first made to a 0.25 inch diameter sample of Stycast $\varepsilon' = 10$ material as before; then the KRS-5 sample was butt-coupled to the Stycast rod and held in place with a single layer of Scotch Magic Mending Tape. The fields around both rods were probed with a metal perturber and the reflections noted. There was no evidence of radiation around the Stycast section; fields were confined to the same region as before. There was some radiation around the KRS-5 rod, but the fields were much stronger very close to the rod (about 1-2 mm from the surface), so that a guide wavelength measurement could be made by sliding a washer along the rod as before. The resulting guide wavelength of 0.74 cm is in good agreement with the theoretical value of 0.71 for an $\varepsilon' = 32$ rod, 0.21 inch in diameter.

The fields around the KRS-5 rod were probed with the short wire probe with essentially the same results as described for the Stycast $\varepsilon' = 10$ rod. Smaller values of reflection were observed at all positions since the fields outside this higher dielectric constant material are substantially weaker and closer to the surface than in the case of the $\varepsilon' = 10$ material.

In order to obtain a direct measurement of the attenuation on the KRS-5 rod, the magnitude of the reflection variation was noted as the washer was moved over a short length of the rod. Since there was some interference to the standing wave pattern from the free space radiation, it was difficult to measure the decrease accurately; an estimate would be a 20% decrease in reflection amplitude in 3 cm of washer motion. This corresponds to a loss tangent of 0.003, in good agreement with our other measurements at X-band.

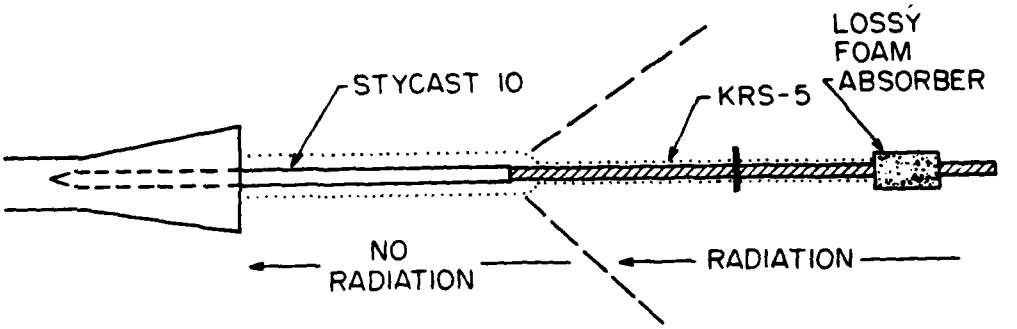

Figure III-5 Butt-coupling arrangement used to excite the KRS-5 rod from a rod of lower dielectric constant. The extent of the HE_{11} fields are shown dotted, while the region where some free space radiation was observed is shown to the right of the dashed line.

D. Later Measurements at 94 GHz

Since butt-coupling to a lower dielectric constant rod had worked at 10 GHz, we attempted to employ a similar technique at 94 GHz. We could not fabricate a 0.5 mm diameter rod from Stycast, since it is a pressed-powder material and very fragile in small cross sections. Furthermore, it is rather lossy at 94 GHz. However, it is easily machined in larger shapes, and it was readily available, so we fabricated a rectangular plug that would slip-fit inside a WR-10 waveguide. The protruding portion of this plug was then tapered (about 3:1) down to 0.5 mm diameter. A short length of KRS-5 fiber was then glued onto this small end. (The loss characteristics of the glue at 94 GHz is unknown.) Despite the unknowns in this scheme, a pattern with a guide wavelength approximately 1/2 of the free space wavelength was observed as a metal perturber was moved along the surface of the fiber. Again, interference from the free space radiation prevented an accurate measurement of the attenuation, but the reflection amplitude variation at the 1/2 wavelength died off in a distance consistant with the value of $\alpha = 1$ per cm calculated from our bulk measurements.

E. Future Dielectric Waveguide Measurements

All indications to date are that the losses in the HE_{11} mode will be too great in KRS-5 to yield a practical flexible waveguide. However, we have observed a mode of propagation on these fibers with much lower loss, of the order of 20 dB/meter. This unidentified mode also seems to be tightly confined to the fiber, and reasonably unaffected by bends of 20 cm radius or so. While 20 dB/meter may still be too high to compete with the value of 3 dB/meter for rigid copper WR-10 guide, there may be some applications in which the guide flexibility outweighs the added loss. In any case, we

intend to identify the field configuration of the mode and measure its properties accurately, comparing with theory if possible.

We also intend to develop further the butt-coupling technique of exciting the HE_{11} mode in KRS-5 fibers and measure the attenuation constant accurately to confirm our bulk loss tangent measurements. We feel that the techniques of coupling into and out of high dielectric constant waveguides will be of value for other (rigid) materials such as GaAs and silicon, and will be required by the dielectric waveguide device research we will undertake for the remainder of the present program.

TABLE III-1

Measurement of Guide Wavelength at 10 GHz

Material	ϵ'	Size (mm)	Shape	HE_{11} Guide Wavelength	
				Experiment (cm)	Theory (cm)
Lucite	2.5	6.3	○	2.9	3.0
Stycast	10	6.3	○	2.2	2.5
Stycast	10	6.3	□	1.7	?
Stycast (*)	20	6.3	□	1.8	not HE_{11}
KRS-5 (**)	32	5.3	○	0.74	0.71

Notes: (*) Lap coupled; produced asymetrical excitation

(**) Butt coupled

REFERENCES FOR SECTION III

III-1. A. E. Popa and R. E. Johnson, Hughes Research Laboratories, Malibu, CA; unpublished data 1978.

IV. THEORY OF DIELECTRIC WAVEGUIDES (E. Schweig)

A. Introduction

Hondros and Debye (Ref. IV-1) and, more recently, Elsasser (Ref. IV-2), and Chandler (Ref. IV-3) have studied a dielectric rod as a structure capable of supporting a "surface wave," that is, an electromagnetic wave which is bound to the surface of the structure; the fields are characterized by an exponential decay away from the surface and a propagation function $\exp(-j\beta z)$. These studies have shown some of the peculiar features of the "surface wave" modes that differ from the modes existing in conventional metallic waveguides:

1. The possibility of a guided mode with no low frequency cutoff;
2. The existence of only a finite number of discrete modes together with a continuous eigenvalue spectrum;
3. The possibility of modes that propagate with a phase velocity less than that of light in free space.

Since the late 1960's optical waveguides in the form of glass fibers have been studied extensively for their applications in optical communication systems (see, for example, the review paper by Gloge (Ref. IV-4)). Such optical waveguides consist of a core surrounded by a cladding of an index of refraction that is somewhat lower than the index of the core. The difference in index is, in practice, on the order of only a few parts in a thousand (hence the name "weakly-guiding fiber"), which leads to significant simplifications in the solution to Maxwell's equations. The results can be summarized in the form of curves that are independent of the actual difference in refractive index as long as it is a small quantity.

At mm-wave frequencies, the wavelength can become comparable in size to the guiding structure, and it is thus necessary to provide for a tighter confinement of the field within the guide ("strongly-guiding fiber"). This is realized by using materials that have a large refractive index difference between the core and the cladding. In such a guide, it is necessary to compute the exact solution to Maxwell's equations for each configuration. Relatively little work has appeared in the literature recently on such strongly-guiding structures compared to the vast literature on weakly-guiding optical fibers.

We will describe in the next paragraphs the theory of circular fibers and the results of some computations on the propagation characteristics and the losses of these fibers. At the end of the section we will give a short description of previous approaches to the problem of solving Maxwell's equations for rectangular dielectric waveguides and even more general cross sections, and the direction we have taken to obtain solutions for these cases.

B. Theory of Dielectric Waveguides with Circular Cross-section and Infinite Cladding

1. Equations

The simplest dielectric waveguiding structure consists of a round fiber that has a core of index n_1 and a radius $\underline{a}$ and is surrounded by an infinite medium of index n_2. This fiber is illustrated in Fig. IV-1. Such a configuration describes exactly the unclad or bare fiber case; in addition, it can serve as a first approximation to the clad, or 3-region fiber if the fields in region 2 die off fast enough so that they are small at the interface between regions 2 and 3.

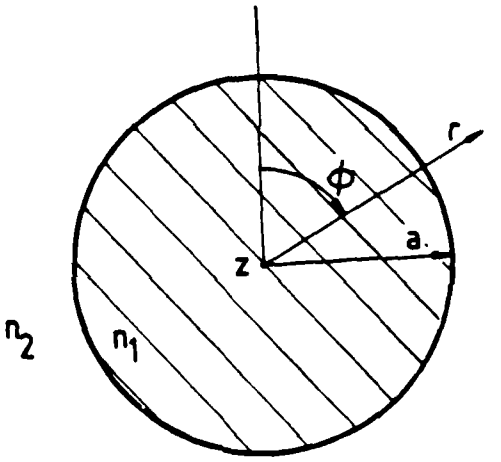

Figure IV-1 Round Fiber with infinite cladding; system of coordinates.

We will consider a time-harmonic solution of frequency ω and a cylindrical system of coordinates (r, ϕ, z), with the z-axis along the fiber axis. At first we will consider all media to be isotropic, homogeneous and lossless; the losses will be incorporated afterwards as a perturbation.

The field components of E and H can be derived from the generating components E_z and H_z (see, for example, Langmuir (Ref. IV-5)); these components are,

in region 1:

$$E_{z_1} = A_E J_m(k_{r_1} r) \cos m\phi$$

$$H_{z_1} = A_H J_m(k_{r_1} r) \sin m\phi \qquad \text{for } r \leq a, \tag{IV-1}$$

and in region 2:

$$E_{z_2} = B_E K_m(jk_{r_2} r) \sin m\phi$$

$$H_{z_2} = B_H K_m(jk_{r_2} r) \sin m\phi \qquad \text{for } r \geq a. \tag{IV-2}$$

All of the field components have a common $\exp(-j\beta z)$ dependence which has been omitted for simplicity. The transverse separation constants k_{r_q} satisfy the relation

$$k_{r_q}^2 = n_q^2 k^2 - \beta^2 \qquad \text{for } q = 1, 2 \tag{IV-3}$$

where k is the wavenumber in free space.

The choice of the radial functional dependence given in Eqs. IV-1 and IV-2 assures the proper behavior of the fields in each region for the modes. The tangential components of E and H must be matched at the interface $r = a$.

This matching then specifies a system of four linear homogeneous equations for the four undetermined factors A_E, A_H, B_E, and B_H. The compatibility condition for this system is the characteristic equation in β for modes propagating in the core, Eq. IV-3. The various modes that are obtained are designated E_{on}, H_{on}, HE_{mn}, and EH_{mn}. The first capital letter indicates the dominant longitudinal field component; the second letter (if any) indicates that the mode is a hybrid, that is, it has both longitudinal electric and magnetic fields. The subscripts designate the order of the mode: m for the angular variation and n for the radial variation.

To describe the solutions, we will use the following abbreviations that are common in the description of optical fibers (Unger, Ref. IV-6); we define a radial phase parameter in the core, u, and a radial attenuation parameter in the cladding, v:

$$u = k_{r_1} a = a\left(n_1^2 - \beta^2\right)^{1/2} \tag{IV-5a}$$

$$v = jk_{r_2} a = a\left(\beta^2 - n_2^2\right)^{1/2} \tag{IV-5b}$$

We also define a normalized frequency V:

$$V = ka\sqrt{n_1^2 - n_2^2} \tag{IV-6}$$

and a normalized propagation constant B

$$B = \frac{(\beta/k)^2 - n_2^2}{n_1^2 - n_2^2} \tag{IV-7}$$

In the particular case of a fiber consisting of a core surrounded by an infinite cladding, we can deduce the partition of power flow between the two media from the characteristic (dispersion) curve of B vs V. If the waveguide incorporates only isotropic and non-dispersive materials, the fraction of the power that is guided within the core is given by Krumbhols, et al. (Ref. IV-7):

$$\rho_{core} = B + \frac{V}{2}\frac{dB}{dV} \qquad \text{(IV-8)}$$

The attenuation of the guided mode is then given by:

$$\alpha = \alpha_1 \rho_{core} + \alpha_2 \rho_{cladding} \qquad \text{(IV-9)}$$

where α_1 and α_2 are complicated functions derived from the characteristic equation. However, if the mode is well confined so that most of the power travels within the core, α_1 is equal to the bulk material attenuation of region 1.

2. Results of Numerical Calculations

A program was written that solves numerically the characteristic equation for a round fiber with an infinite cladding. The results are presented in Figs. IV-2,3,4 in terms of the normalized parameters V and B. Figure IV-2 corresponds to a core of Teflon surrounded by air, and Figs. IV-3 and IV-4 correspond to a core of KRS-5 surrounded by air and Teflon respectively. The succession of the various modes, that is, the order in which they turn on as frequency is increased, remains the same in all three cases; but as the index of the core is increased the phase parameter corresponding to the HE and E modes remains very small until a higher value of frequency (V) is reached.

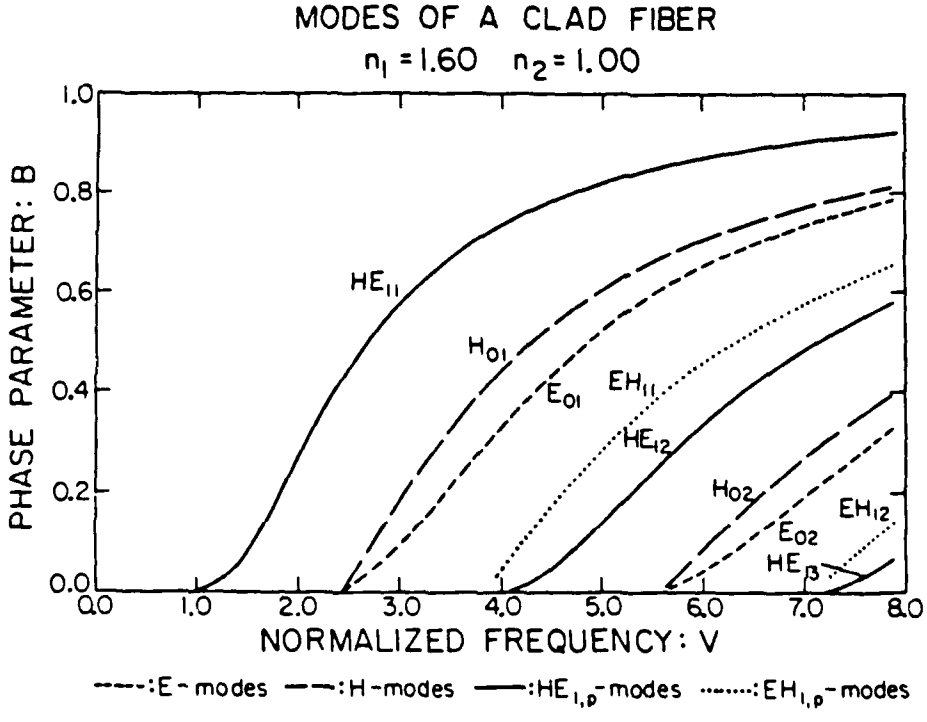

Figure IV-2 Modes of a round fiber with infinite cladding

core: $n_1 = 1.60$ (Teflon

cladding: $n_2 = 1.00$ (air)

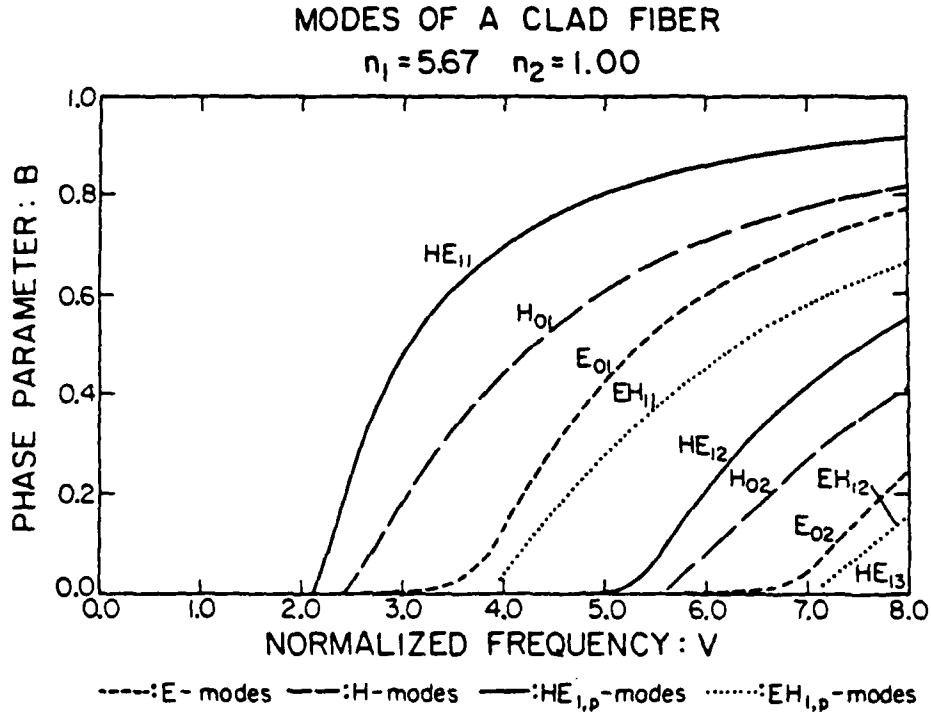

Figure IV-3 Modes of a round fiber with infinite cladding

core: $n_1 = 5.67$ (KRS-5)

cladding: $n_2 = 1.00$ (air)

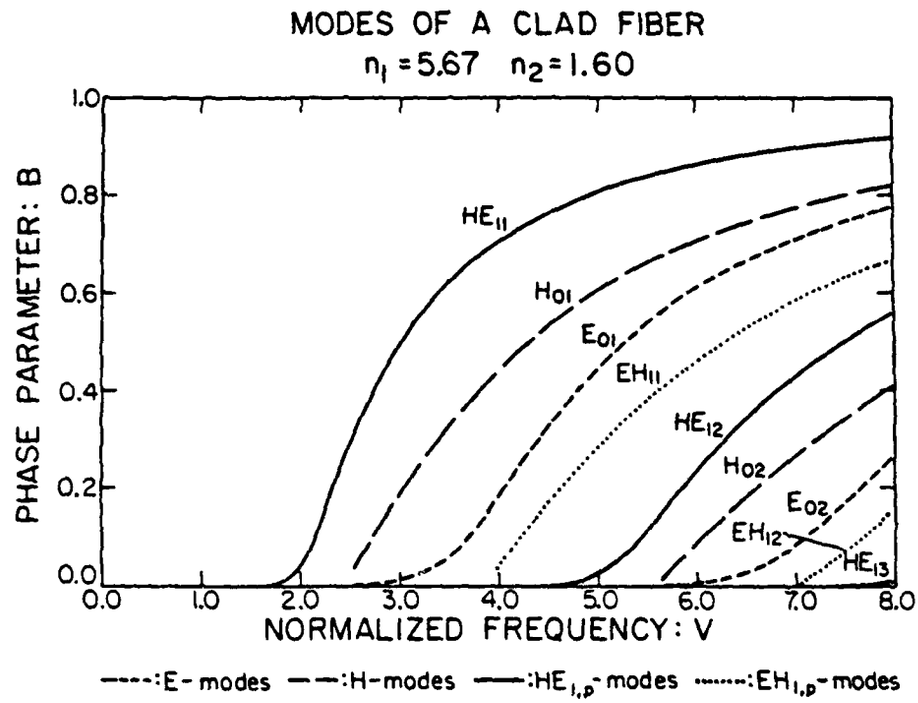

Figure IV-4 Modes of a round fiber with infinite cladding

core: $n_1 = 5.67$ (KRS-5)

cladding: $n_2 = 1.60$ (Teflon)

For most millimeter wave applications the waveguide should be used in a single mode configuration. It is therefore important to determine the frequency range over which only the lowest order HE_{11} mode can exist. This is similar to the useful frequency range of ordinary metallic "dominant mode" waveguide. Unlike the dominant mode in metallic waveguide, the HE_{11} has no low-frequency cutoff; as the frequency is decreased, more and more of the power will flow outside of the core, resulting in weak guiding or "loose confinement." We will consider the HE_{11} mode to be strongly guiding or "closely confined" when at least 90% of the power is propagating within the core (an arbitrary definition); this defines the lower frequency limit of the single mode range. The high-frequency limit of single mode operation occurs when the next mode is cut on, which occurs for a fixed value of V = 2.38 in all cases. Figures IV-5 to IV-8 show the dispersion characteristic and power distribution in the different fiber combinations considered above. If the core has a high index of refraction, the HE_{11} mode will turn on very rapidly, as illustrated by Figs. IV-5 and IV-6. Figures IV-7 and IV-8 show this rapid increase on an expanded scale. Note that for the KRS-5/air fiber combination shown in Figure IV-7 there is a region of strong guiding in single mode operation, for V = 2.2 to V = 2.38. However, for the KRS-5/Teflon fiber shown in Figure IV-8, the next mode cuts on before strong guiding (90% power in the core) occurs. The reduction in the difference in index between core and cladding slows the rise in the fraction of the power carried by the core.

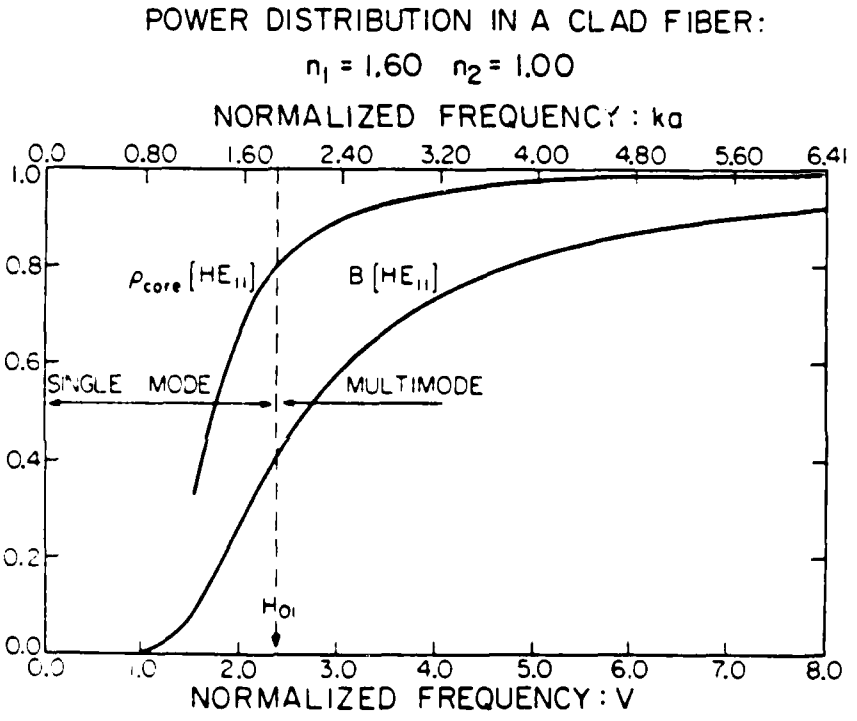

Figure 5 Dispersion characteristic and power distribution of round fibers with infinite cladding

core: $n_1 = 1.60$

cladding: $n_2 = 1.00$

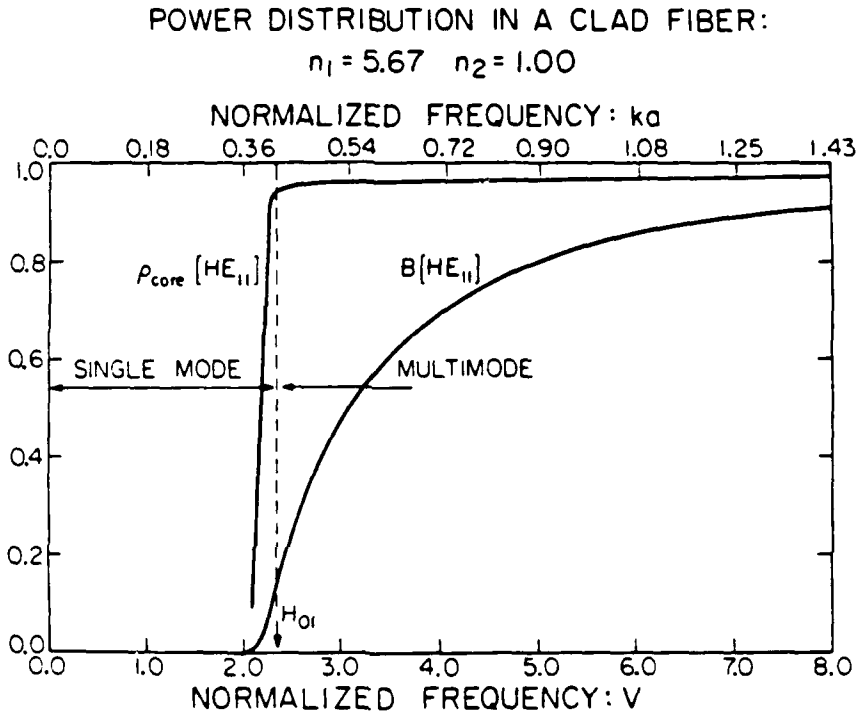

Figure IV-6 Dispersion characteristic and power distribution

a round fiber with infinite cladding

core: $n_1 = 5.67$

cladding: $n_2 = 1.00$

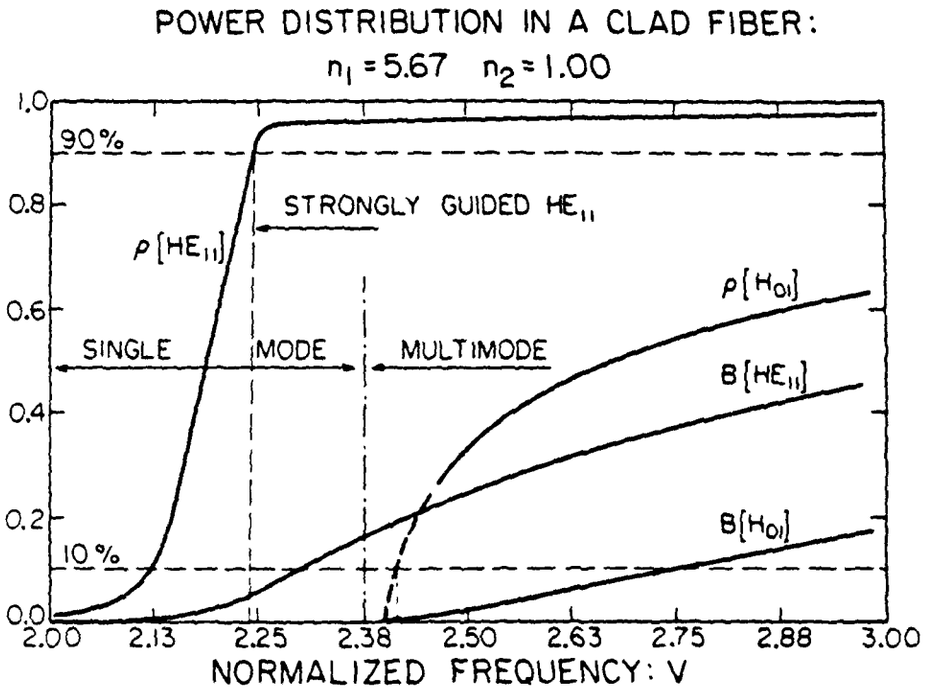

Figure IV-7 Dispersion characteristic and power distribution of a round fiber with infinite cladding (enlarged scale)

core: $n_1 = 5.67$

cladding: $n_2 = 1.00$

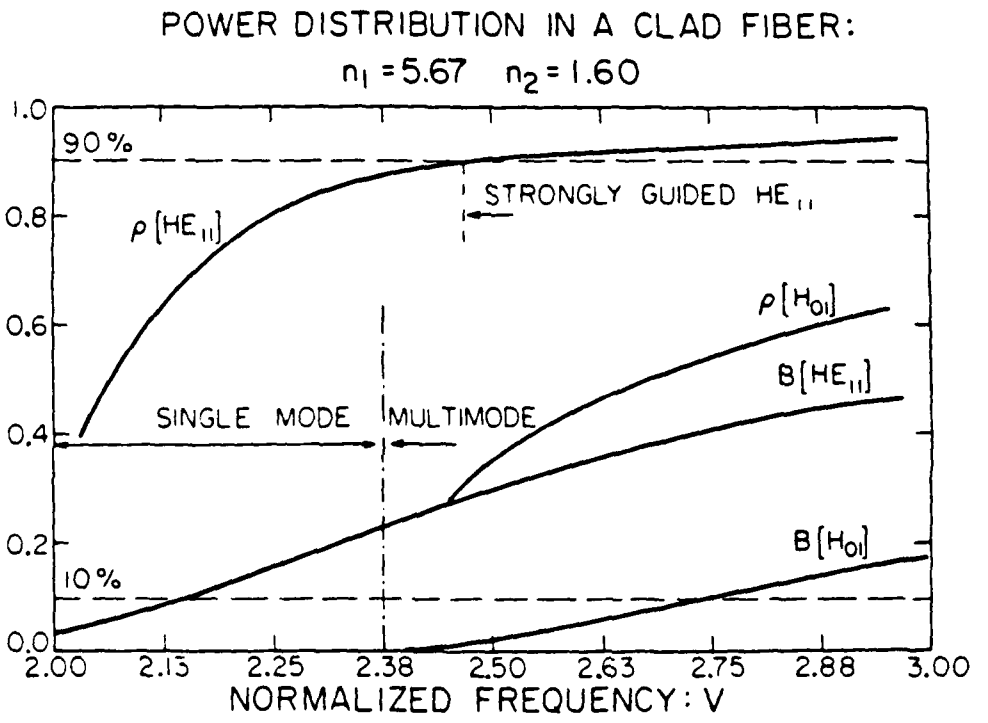

Figure IV-8 Dispersion characteristic and power distribution of a round fiber with infinite cladding (enlarged scale)

core: $n_1 = 5.67$

cladding: $n_2 = 1.60$

3. Losses

The total propagation losses for a dielectric waveguide result from the dielectric losses in the core and cladding and from the bending losses:

$$\alpha = \alpha_{core} + \alpha_{cladding} + \alpha_{bending} \qquad \text{(IV-10)}$$

where α is the real part of the complex propagation constant $\gamma = \alpha + j\beta$.

It is assumed that the dielectric losses are sufficiently small that the field distribution in the modes is identical to the distribution computed in a lossless case; we then have:

$$\alpha_{core} = \alpha_M \rho_{core} \qquad \text{(IV-11)}$$

$$\alpha_{cladding} = \alpha_M (1-\rho_{core}) \qquad \text{(IV-12)}$$

where α_M corresponds to the real part of the propagation constant of a plane wave in the bulk material, as given by

$$\alpha_M \simeq \frac{\pi}{\lambda_o} \sqrt{\varepsilon'_r} \tan \delta \qquad \text{(IV-13)}$$

and ρ_{core} is the fraction of the total power that is guided within the core.

Several authors have proposed formulas for computing the bending losses of dielectric waveguides. Neuman, et al. (Ref. IV-8, 1975) has shown that these formulas can be reduced to a common expression:

$$\alpha_R \simeq \frac{1}{R} \exp\left[- \frac{1}{6\pi^2} \frac{(R/\lambda_o)}{(r_o/\lambda_o)^3} \right] \qquad \text{(IV-14)}$$

where R is the radius of curvature, λ_o is the wavelength in the outer medium, and r_o is the extension of the field in this region. (The fields, outside of the core behave like $K_1(r/r_o)$, which can be approximated by an exponential decay $\exp(-r/r_o)$.)

We may now compute the fiber losses for three cases of practical interest, namely those fiber designs that have an attenuation comparable to metallic waveguides.

a. KRS-5/air waveguide. For the sake of comparison, we determine the radius a of the core so that the dielectric losses correspond to the losses of conventional metallic waveguides at 94 GHz:

$$\alpha_{core} = 3 \text{ dB/m} = 3.45 \times 10^{-4} \text{ mm}^{-1}$$

For very small ka, we can approximate the dispersion relation by

$$B \simeq \frac{1.26}{V^2} \exp[-D/V^2] \qquad \text{(IV-15)}$$

where $D = 1 + (n_1/n_2)^2$ (Unger, Ref. IV-5, 1975). Also, we have seen earlier that the power distribution is given by

$$\rho_{core} = B + \frac{V}{2} \frac{dB}{dV} \qquad \text{(IV-16)}$$

and therefore,

$$\rho_{core} \simeq \frac{1.26}{V^4} D \exp(-D/V^2) \qquad \text{(IV-17)}$$

Because $\alpha_{core} = \rho_{core}\, \alpha_M$ this value of α_{core} corresponds to $\rho_{core} = 3.1 \times 10^{-3}$ for KRS-5 (see Table IV-1). Knowing the value of ρ_{core}, we can now solve Eq. (IV-17) by successive iterations and find that V = 1.9. From (IV-15) and the definition of B we deduce for the propagation constant: $\beta/k = 1.0006$, with $k = 1.97\ mm^{-1}$ at 94 GHz. In order to compute the radiation losses, we must know r_o, the extension of the fields outside of the core, in the air. From the theory of a fiber with infinite cladding, we have

$$1/r_o = (\beta^2 - k^2)^{1/2} \qquad \text{(IV-18)}$$

and therefore, $r_o = 21.2$ mm. The bending losses, for a bending radius R = 200 mm, become $\alpha_R = 5.0 \times 10^{-3}$, and for R = 600 mm, $\alpha_R = 2.2 \times 10^{-4}$, about 3 dB/meter or the same as the dissipative losses in WR-10 metallic waveguide.

b. Teflon/air waveguide. Using the same steps as in case a, we obtain successively

$$\rho_{core} = 0.12$$

$$V = 1.25$$

$$a = 0.51 \text{ mm}$$

$$\beta/k = 1.06$$

$$r_o = 1.44 \text{ mm}$$

$$\alpha_R = 5.1 \times 10^{-8}\ mm^{-1} \text{ for } R = 200 \text{ mm}$$

$$\alpha_R = 1.7 \times 10^{-18}\ mm^{-1} \text{ for } R = 600 \text{ mm}$$

These two cases demonstrate that the advantage of a high-index core would

be to provide a better confinement of the fields inside the core. But this advantage is practical only if the core material is low loss. KRS-5 is too lossy, and in order to achieve a small dielectric loss, most of the power would actually travel outside of the core; such a fiber suffers then from high bending losses because the mode is loosely confined. Teflon has a lower dielectric loss than KRS-5 so to obtain losses comparable to metal waveguides, we can guide 12% of the power inside the core. This confinement is already sufficient to lower the bending losses by several orders of magnitude.

c. KRS-5/Teflon/air waveguide. The losses in this case are worse than the losses in case a and b. We must now add to the dielectric losses in the KRS-5 core the losses in the Teflon cladding. The cladding in all practical cases will be very large so that the fields at the interface Teflon/air are negligible, thus the losses in the Teflon will be essentially the bulk losses and it will not be possible to achieve a dielectric loss of 3 dB/m, no matter how small we choose the core. Also the guiding properties of the KRS-5 core are degraded because the difference in index of refraction between the core and the outer medium is now decreased (see discussion of the propagation characteristics, earlier in part IV).

We must remark that in case a and b the outer medium is indicated as "air," but a practical realization will involve the use of a foamed material that will approximate the dielectric properties of air: $\varepsilon_r' \simeq 1$ and very small losses. This is required in order to supply mechanical support and prevent the fields from coupling with external objects.

Finally, we must conclude that KRS-5 is not a suitable material for a closely confined HE_{11} dielectric waveguide because of its high losses. Teflon can be used (and is actually used in various applications) but only for short lengths.

C. Dielectric Waveguides of Rectangular Cross-section

The problem of a dielectric waveguide with a rectangular core cannot be solved exactly. Marcatili suggested an approximate solution by satisfying only some of the boundary conditions and neglecting the corner regions. He compared the accuracy of his solutions to numerical computations done by Goell and found out that, for weakly-guiding cores (the index difference between core and cladding is small) and far from cutoff, the approximate solution gives good results. Goell used a numerical method based upon the point-matching technique, that consists of expanding the fields in the modes of a simple geometry. More recently, C. Yeh applied the finite-element method to the solution of Maxwell's equations for an arbitrarily-shaped dielectric waveguide. These methods, their assumptions and limitations will be described in the next sections. The last section will be devoted to a short analysis of the finite-difference technique that we intend to use for our computations of the modes in rectangular dielectric waveguides.

(1) Marcatili's approach (Ref. IV-9)

Marcatili assumes that the power is well confined inside the core; he ignores the corner regions so that he matches the field inside the core with the fields existing in the cladding only along the boundaries that form the side of the rectangular core region. The index of refraction of the core is supposed to be very close to the index of the cladding; therefore the modes must be quasi-plane waves and are designated $E^{x}_{m,n}$, where the superscript indicates the direction of polarization. In each region a certain behavior is assumed for the components of the fields (see Fig. IV-9). The fields are then matched at the boundaries in order to give a resulting characteristic equation. In this process, however, Marcatili neglects the field components that are not dominant. He then obtains simple characteristic equations. The dispersion curves agree well with the results of numerical

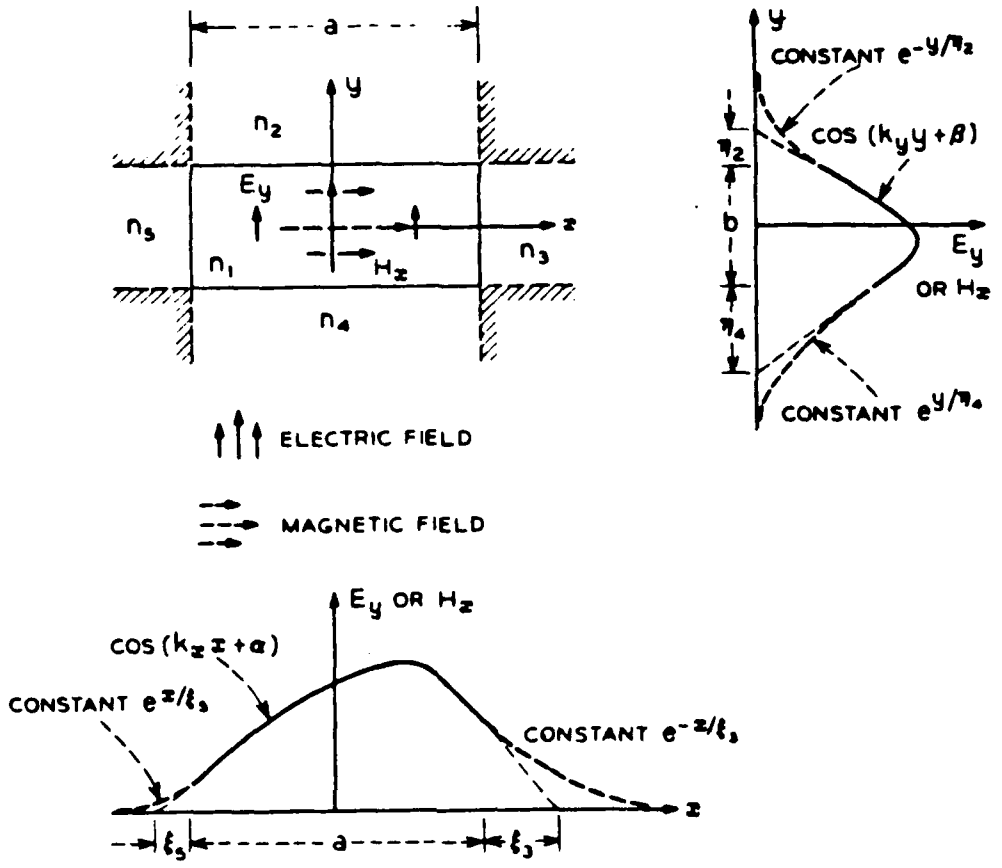

A.1 E^y_{pq} *Modes: Polarization Along y*

The field components in the νth of the five areas:

$$H_{\nu\nu} = \exp(-ik_z z + i\omega t)\begin{cases} M_1 \cos(k_x x + \alpha)\cos(k_y y + \beta) & \text{for } \nu = 1 \\ M_2 \cos(k_x x + \alpha)\exp(-ik_{y2} y) & \text{for } \nu = 2 \\ M_3 \cos(k_y y + \beta)\exp(-ik_{x3} x) & \text{for } \nu = 3 \\ M_4 \cos(k_x x + \alpha)\exp(ik_{y4} y) & \text{for } \nu = 4 \\ M_5 \cos(k_y y + \beta)\sin(k_{x5} x + \gamma) & \text{for } \nu = 5 \end{cases}$$

$$H_{z\nu} = 0$$

$$H_{x\nu} = -\frac{i}{k_c}\frac{\partial^2 H_{z\nu}}{\partial x\,\partial y}$$

Figure IV-9 Marcatili's approach to the solution of a rectangular dielectric waveguide

computations (Goell and Yeh) except near cutoff when the power is not confined. Because of the various assumptions involved, the method cannot be extended for the case when the core has a high index of refraction compared to the cladding region. Also the analysis becomes very complicated when additional layers are added.

(2) Goell's numerical computations (Ref. IV-10)

Goell expends the solution of the wave equations in terms of a finite series of the modes of a round fiber, weighted by unknown coefficients. These coefficients are then determined by matching the fields at a finite number of points disposed along the boundary. The number of terms in the expansion that are needed is on the order of 3-5, for any practical accuracy. However the solution does not provide any physical insight into the problem. This method is hard to generalize for more complicated geometries. Also, according to C. Yeh (Ref. IV-11) the results are accurate only when the aspect ratio is close to unity (almost-square waveguide).

(3) Finite-elements (C. Yeh, Ref. IV-12, 13)

The finite-element method, well known to mechanical engineers, was applied by C. Yeh to the problem of wave propagation along arbitrarily shaped inhomogeneous optical waveguides. It is a purely numerical method based upon the exact Maxwell's equations. It consists of dividing each homogeneous region into subdomains of triangular shape and assuming that the solution will vary linearly over such a triangular domain. The problem is then reduced to computing the eigenvalue of a large matrix; one eigenvalue of this matrix corresponds to the propagation constant of a given mode and the corresponding eigenvector determines the field values at the center of each triangular domain.

The method is somewhat complicated in its formulation, especially in the treatment of the boundary conditions between two different homogeneous regions.

(4) Finite differences (this work)

It was felt that a computer program for determining the characteristics of dielectric waveguides of (somewhat) arbitrary shape would be very useful. One of its uses would be to study the properties of rectangular dielectric waveguide when the core regions has a high index. Some recent papers (see for example Ref. IV-14) present computations based on Marcatili's formulas, but without proper considerations of the stringent limitations of this analysis. Marcatili assumed that the index step between core and cladding was so small that modes become quasi-plane waves. For a large difference in index, the modes must become more complex hybrid modes, having both longitudinal electric and magnetic fields. The exact mode pattern becomes a very important characteristic in the millimeter wave range because the active devices that can be integrated with the waveguide are sensitive to the orientation of the electric field. We are developing a computer program based upon the finite difference method. This method is conceptually very simple. A discrete grid is defined over the waveguide region and Maxwell's equations are then transformed into difference equations. The problem is then to solve for the eigenvalues of a matrix. The eigenvalues of this matrix correspond to the propagation constants of various modes and the eigenvectors are the field values at the mesh points. The finite-difference method is, from a numerical point of view, somewhat less efficient than finite-elements. However, we believe that this can be corrected using numerical convergence algorithms.

TABLE IV-1

Dielectric Properties Used in Waveguide Calculations (f = 94 GHz)

Material	ϵ'_r	Tan δ	α_M (mm^{-1})
KRS-5	32	2×10^{-2}	1.11×10^{-1}
Teflon	2.1	2×10^{-3}	2.86×10^{-3}

REFERENCES FOR SECTION IV

IV-1. E. Hondros and P. Debye, "Elektromagnetischen Wellen on Dielektrischen Drahten," Ann. Phys., vol. 32, pp. 465–476 (1910).

IV-2. W. Elasser, "Attenuation in a dielectric circular rod," J. Appl. Phys., vol. 20, pp. 1193-1196 (1949).

IV-3. C. Chandler, "Investigation of dielectric rod as waveguide," J. Appl. Phys., vol. 20, pp. 1188-1192 (1949).

IV-4. E. Gloge, "Weakly guiding fibers," Appl. Opt., vol. 10, pp. 2252-2258 (1971).

IV-5. R. V. Langmuir, ELECTROMAGNETIC FIELDS AND WAVES, McGraw-Hill, New York (1961).

IV-6. H. G. Unger, PLANAR OPTICAL WAVEGUIDES AND FIBERS, Clarendon Press, Oxford (1977).

IV-7. D. Krumbholz, E. Brinkmeyer, and E.-G. Neumann, "Core/cladding power distribution, propagation constant and group delay: simple relation for power-law graded-index fibers," JOSA, vol. 70, pp. 179-183 (1980).

IV-8. E.-G. Neumann and H.-D. Rudolph, "Radiation from bends in dielectric rod transmission lines," IEEE Trans. MTT, vol. MTT-23, pp. 142-149 (1975).

IV-9. E. A. J. Marcatili, "Dielectric rectangular waveguide and directional coupler for integrated optics," BSTJ, vol. 48, pp. 2071-2102 (Sept. 1969).

IV-10. J. E. Goell, "A circular-harmonic computer analysis of rectangular dielectric waveguides," BSTJ, vo-. 48, pp. 2133-2160 (Sept. 1969).

IV-11. C. W. Yeh, "Optical waveguide theory," IEEE Trans. Circ. and Syst., vol. 26, pp. 1011-1019, 1979.

IV-12. C. Yeh, S. B. Dong and W. Oliver, "Arbitrarily shaped inhomogeneous optical fibers on integrated optical waveguides," J. Appl. Phys., vol. 46, pp. 2125-2129 (1974).

IV-13. C. Yeh, K. Ha, S. B. Dong, and W. P. Brown, "Single mode optical waveguides," Appl. Opt., vol. 18, pp. 1490-1504 (1979).

IV-14. C. H. Lee, P. S. Mok and A. P. DeFazo, "Optical control of mm-wave propagation in dielectric waveguides," IEEE J. Quant. Electron., vol. QE-16, pp. 277-288 (1980).

V. GENERAL GUIDELINES FOR THE DESIGN OF MULTILAYER CYLINDRICAL DIELECTRIC WAVEGUIDES (A. E.-T. Chiou)

A. Introduction

In this section we examine the nature of the modes that propagate along a multilayer cylindrical dielectric waveguide. Rather than ask for a complete solution to the problem, we derive a simple relation among the values of the dielectric constants of the various layers that will indicate whether the waveguide will have large or small radiative losses due to bending or interference with external objects.

To obtain a simple relation it is necessary to make mathematical approximations that may cast some doubt on the validity of the final result; however, the approximations required to make the problem mathematically tenable. We assume that all dielectric materials are lossless, and, further that the guide itself is "lossless" in the sense that we constrain the guide propagation constant β to be real. (Waves propagate along the guide as $\exp(-j\beta z)$.) We know that in reality the dielectric materials will exhibit some loss, which would require us to consider complex values of β. Even for lossless dielectrics, β can be complex if the guide radiates into its surroundings. Thus, allowing only real values for β is, strictly speaking, incorrect. What we hope for here is that the general conclusions about the nature of the field solutions (that is, whether they are largely radiative-like or largely evanescent) will not change with small values of dielectric loss or actual radiation. The recent publication of experimental results by Yamamoto (Ref. V-10) gives us some confidence that the simple relation is useful, since it is able to explain his results.

B. Background

The theory and applications of dielectric waveguides have appeared in the literature since the turn of the century (V-1,2). Almost all of the existing papers (for example, Refs. V-1 through V-10) deal exclusively with one or two specific configurations with a specific application in mind. This paper deals with the general behavior common to all members of a class which we call multi-layer coaxial dielectric waveguides. A very general multilayer coaxial dielectric waveguide is shown in Fig. V-1. All the dielectric layers are assumed to be lossless, i.e., the relative permittivities $\varepsilon_i (i = 1,n)$ are all real. Some of the specific members of such a general system are shown in Figure V-2. For efficient guiding of an electromagnetic wave, there are two features that are generally desirable:

1. The fields (power) in the outermost region should be kept as weak as possible. In other words it should vanish as fast as possible as one moves away from the axis;

2. In case the dielectrics are lossy, the fields (power) within the media with high dielectric loss should be kept weak. Condition 1 ensures that the guided wave will be weakly coupled to the external world so that the radiation loss will be small (due to either bending or interaction with objects in the vicinity such as mounting hardware. Condition 2 ensures that the overall dielectric loss is small.

C. Analysis

Consider a cylindrical coordinate system (r, ϕ, z) wgere tge z axis coincides with the axis of the coaxial system; the general solution for a wave propagating along the z-direction (i.e., with z and time dependence given by $\exp[j(\omega t - \beta z)]$) can be obtained by the standard methods (V-11).

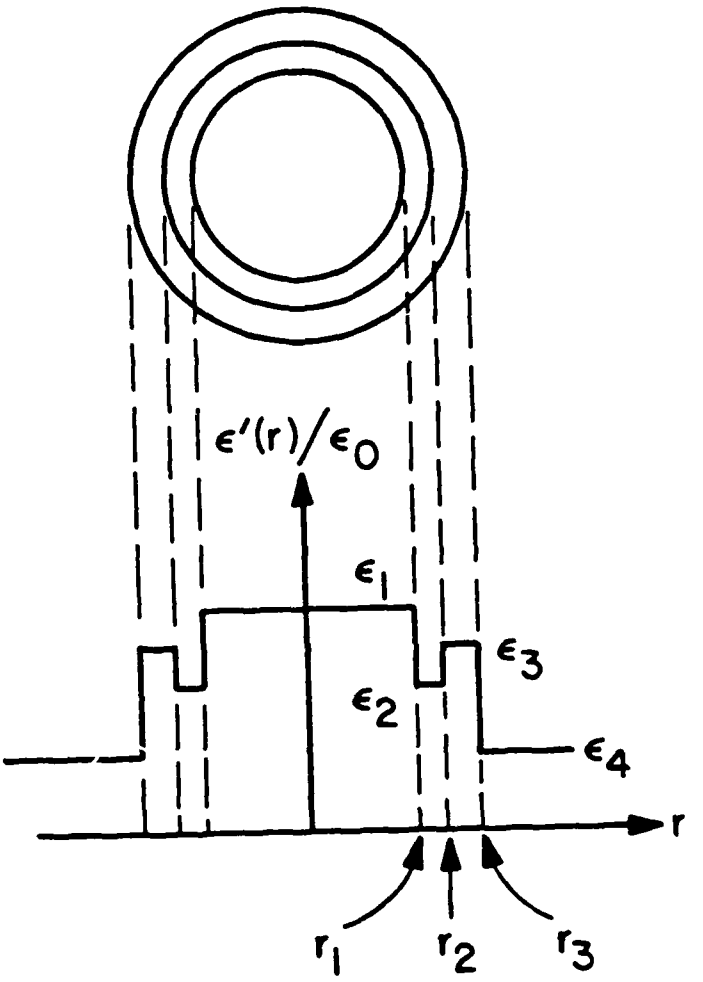

Figure V-1 Multilayer coaxial dielectric waveguide; all ϵ_i are real for lossless dielectrics.

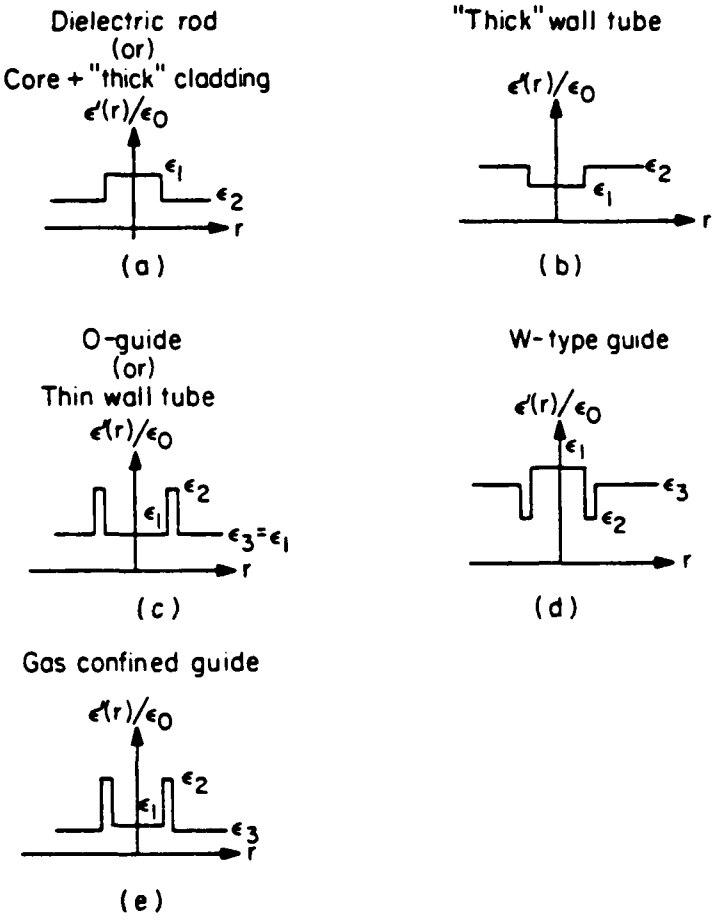

Figure V-2 Some specific systems that have been discussed in the literature

In general we can express it as follows. Inside each layer i:

$$E_{zi} \simeq \left\{A_i J_n(k_i r) + B_i N_n(k_i r)\right\} \cos(n\phi) \exp[j(\omega t - \beta z)] \qquad \text{(V-1)}$$

$$H_{zi} \simeq \left\{C_i J_n(k_i r) + D_i N_n(k_i r)\right\} \sin(n\phi) \exp[j(\omega t - \beta z)] \qquad \text{(V-2)}$$

with

$$k_i^2 + \beta^2 = \varepsilon_i k_o^2 \qquad \text{(V-3)}$$

where

J_n = Bessel function of order n

N_n = Neumann function of order n

k_i = radial wavenumber in medium i

$\beta = 2\pi/\lambda_g$ = axial wavenumber

λ_g = guide wavelength

$k_o = 2\pi/\lambda_o$ = wavenumber in free space

$\sqrt{\varepsilon_i}\, k_o = 2\pi/\lambda_i$ = wavenumber in the unbounded medium with relative permittivity = ε_i

All the other field components, namely E_r, E_ϕ, H_r, H_ϕ, can be expressed in terms of E_z and H_z. If we assumed that all the dielectrics are lossless, then both ε_i and β are real, while k_i can be either real or imaginary (subject to some constraints to be discussed in the following section). When k_i takes on imaginary values, it is appropriate to deal only with real numbers by simply expressing it as $k_i = j\delta_i$ (δ_i is real), so that Eqs. V-1 to V-3 become

$$E_{zi} = [A_i I_n(\delta_i r) + B_i K_n(\delta_i r)] \cos(n\phi) \exp[j(\omega t - \beta z)] \qquad \text{(V-4)}$$

$$H_{zi} = [C_i I_n(\delta_i r) + D_i K_n(\delta_i r)] \sin(n\phi) \exp[j(\omega t - \beta z)] \qquad (V-5)$$

$$-\delta_i^2 + \beta^2 = \varepsilon_i k_o^2 \qquad (V-6)$$

The major difference in the two cases lies in the fact that the functions J_n and N_n have oscillatory behavior, while the functions I_n and K_n are of exponential nature. Since the values of the functions $N_n(r)$ and $K_n(r)$ are infinite at $r = 0$, they are not allowed in the expression for the field in the inner-most region. For the same reason, the functions $I_n(r)$ should be excluded from the solution for the outer-most region.

If we consider only the inner-most region and the outer-most region and forget about the intermediate region, it turns out that there are four possible combinations of solutions as shown in Fig. V-3. Note that all the functions, $J_n(kr)$, $J_n'(kr)$, $N_n(kr)$ and $N_n'(kr)$ behave asymptotically like $\exp[\pm jkr]/\sqrt{r}$, which describes cylindrical wave propagation. The fields in the outer-most region for case (II) and case (IV) in Fig. V-3 are of this form and imply that the field energy is very poorly confined within the guide due to the outward radiation loss. These are known as radiation modes. For case (I) and case (III) the fields in the outer-most region decay exponentially as r increases. The waves in these cases are confined largely inside the guide and propagate along the axis of the guide. These are known as the guided modes. If we compare case (I) and case (III), it is obvious that fractional energy in the inner-most region for case (I) is, in general, larger than that for case (III), and case (I) is the most desirable (efficient) case of the four for wave confinement.

The story changes when the dielectric loss of the media is significant. As a matter of fact, if any one of the ε, say ε_m is complex, then the axial propagation constant β can no longer be real because the dielectric loss will

unavoidably introduce a decay of the field along the axial propagation direction. It follows from (V-3) that <u>all</u> the k_i (not just the one corresponding to the medium m) become complex. Note that when $k = k' + jk''$, $[J_n(kr), N_n(kr)] \sim \exp[\mp j(k' + jk'')r]/\sqrt{(k' + jk'')r}$. The dielectric loss, therefore, introduces an exponential decay factor in the r dependence in the field expression and the outward radiation becomes an evanescent field. If the loss is sufficiently large, this additional factor will then force the field to decay fast enough as r increases, so that the field energy confinement is improved. It follows that operating a waveguide in modes illustrated in case (II) and case (IV) is sensible only if one or more dielectric media are sufficiently lossy. The "thick wall tube" (Ref. V-7) and "O-guide" (Ref. V-8) are examples of dielectric waveguides with lossy dielectrics operating under the condition described above. Strictly speaking, when one or more dielectric media are lossy, the division of solutions into the four simple cases as shown in Fig. V-3 becomes somewhat vague.

D. <u>Constraints on Radial Wave-Numbers</u>

For a general multi-layer dielectric waveguide with lossless dielectric, if ε_m is the largest of all, ε_i, then

(i) $(\lambda_o/\lambda_g) \leq \sqrt{\varepsilon_m}$;

(ii) k_m can only be real

That is, the field expression inside the medium with the maximum permittivity can only be oscillatory. We cannot have a guided wave propagating with a phase velocity smaller than that of the wave in the "slowest" medium. Thus, if $\varepsilon_m < \varepsilon_i$ for all $i \neq m$, then $v_g < v_m$ is unphysical. (v_g is the phase velocity of the guided wave, and v_m is the phase velocity of a wave in the unbounded medium with permitivity ε_m.) Hence, $v_g \geq v_m$ and therefore

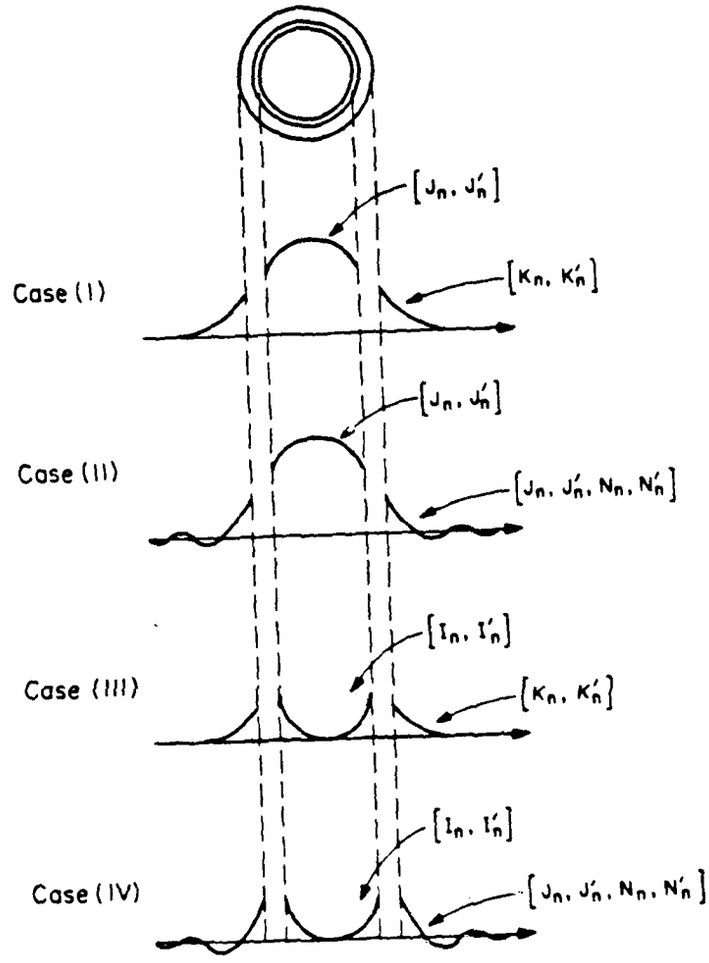

Figure V-3 Four possible combinations of solutions

$\lambda_g \geq \lambda_m = \lambda_o/\sqrt{\varepsilon_m}$. From this it follows that

$$\varepsilon_m \geq (\lambda_o/\lambda_g)^2 \tag{V-7}$$

From Eq. V-3 we have

$$k_m^2 = \varepsilon_m k_o^2 - \beta^2$$

$$= \varepsilon_m(2\pi/\lambda_o)^2 - (2\pi/\lambda_g)^2 = \left(\frac{2\pi}{\lambda_o}\right)^2 \cdot \left[\varepsilon_m - \left(\frac{\lambda_o}{\lambda_g}\right)\right]^2 \tag{V-8}$$

and from Eqs. V-7 and V-8, we have $k_m^2 \geq 0$ or k_m is real. For any other "i" with $\varepsilon_i < \varepsilon_m$ there exists no such restriction. Since the relation

$$k_i^2 = (2\pi/\lambda_o)^2\left[\varepsilon_i - \left(\frac{\lambda_o}{\lambda_g}\right)^2\right] \tag{V-9}$$

holds for any i, it follows that k_i can be either real or imaginary depending on whether $(\lambda_o/\lambda_g)^2$ is less than or greater than ε_i.

The results of the analysis given above can be illustrated schematically as shown in Fig. V-4. For example, at point a where $(\lambda_o/\lambda_g)^2 = a < \varepsilon_2 < \varepsilon_1 < \varepsilon_m$, we have

$(k_1/k_o)^2 = +(\varepsilon_1 - a)$ or $k_1 = k_o\sqrt{\varepsilon_1 - a}$ is real

$(k_2/k_o)^2 = +(\varepsilon_2 - a)$ or $k_2 = k_o\sqrt{\varepsilon_2 - a}$ is real

$(k_m/k_o)^2 = +(\varepsilon_3 - a)$ or $k_m = k_o\sqrt{\varepsilon_m - a}$ is real

at point b where $(\lambda_o/\lambda_g)^2 = b$ such that $\varepsilon_2 < b < \varepsilon_1 < \varepsilon_m$, we have

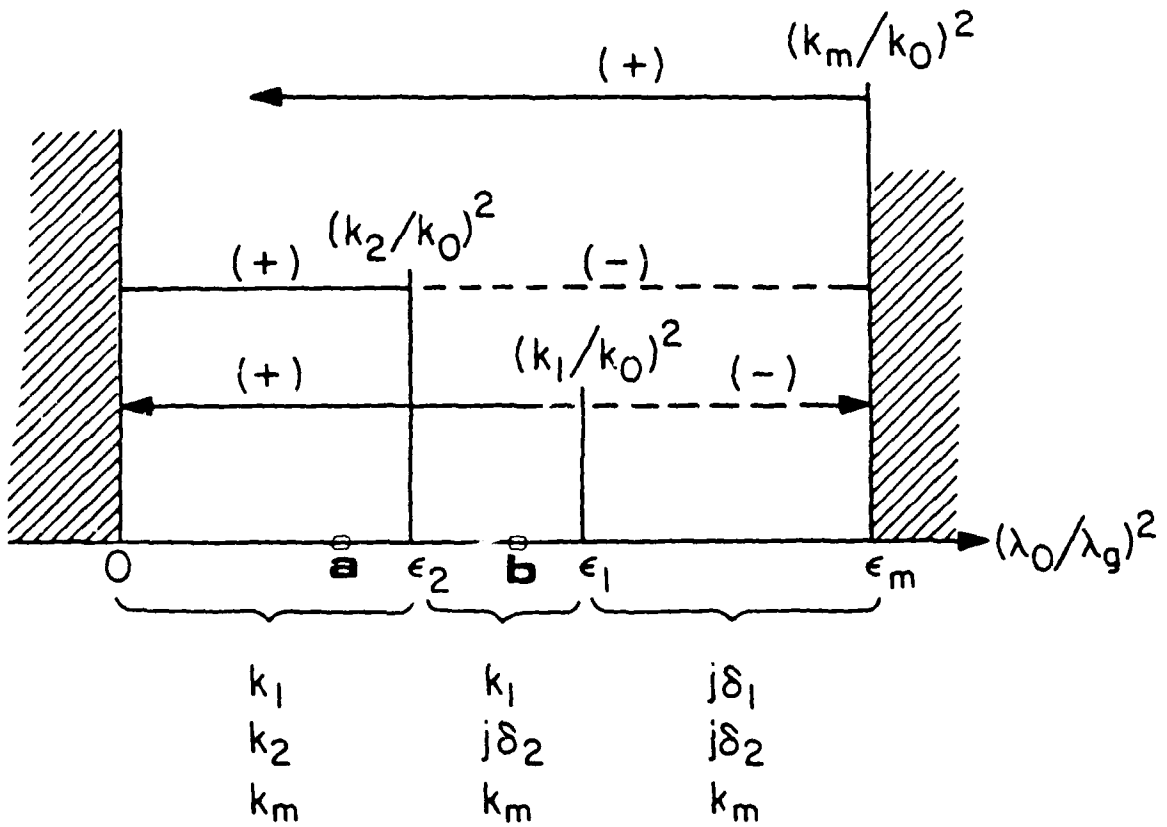

Figure V-4 Illustration of constraints on radial wave number for a coaxial dielectric waveguide with $\epsilon_2 < \epsilon_1 < \epsilon_m$

$$(k_1/k_o)^2 = (\varepsilon_1 - b) \qquad \text{or} \qquad k_1 = k_o\sqrt{\varepsilon_1 - b} \text{ is real}$$

$$(k_2/k_o)^2 = -(b - \varepsilon_2) \qquad \text{or} \qquad k_2 = j\delta_2 = jk_o\sqrt{b - \varepsilon_2} \text{ is imaginary}$$

$$(k_m/k_o)^2 = +(\varepsilon_m - b) \qquad \text{or} \qquad k_m = k_o\sqrt{\varepsilon_m - b} \text{ is real}$$

Application of the analysis to the O-guide (Ref. V-5) (a thin-walled dielectric tube with air inside and out) and the gas-confined guide (Ref. V-10) (a thin-walled tube with air outside and higher dielectric constant gas, e.g., butane, inside) is shown in Fig. V-5 with the results tabulated side by side at the bottom of the figure.

As already explained in the previous section, if the dielectric loss is insignificant, field solutions corresponding to case (II) and case (IV) in Fig. 3 lead to the radiation modes. Only the solutions corresponding to case (I) and case (III) result in the guided modes. It is obvious that, quantitatively speaking, the gas-confined guide which allows field solution corresponding to case (I) while operating in region AB (see Fig. V-5) is better than the O-guide which can at best be operated in the region AC corresponding to case (III). This is essentially the result of the quantitative analysis given by Yamamoto (Ref. V-10).

E. A Review of Literature

If we apply the analysis described above to each of the specific configurations illustrated in Fig. V-2 that have appeared in the literature, we see that the dielectric rod (Fig. V-2a) (Ref. V-3,4,6), the W-type guide (Fig. 2d) (Ref. V-9) and the gas confined guide (Fig. V-2e) (Ref. V-10) can be operated in a region such that the field distribution take the form of Fig. V-3a. As a consequence they are in general

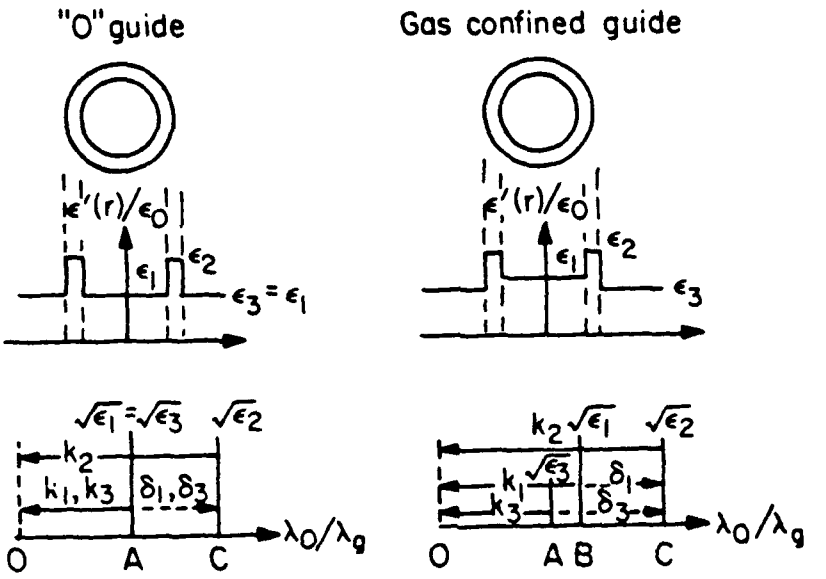

Operating point	Solution
OA	case(II)
AC	case(III)

Operating point	Solution
OA	case (II)
AB	case (I)
BC	case (III)

Figure V-5 O-guide v.s. gas confined guide

related or similar counterparts that do not allow such solution. We also see that as far as the guided modes are concerned, the thick wall tube (Fig. V-2b) (Refs. V-4,7) and the O-guide (Fig. V-2c) (Refs. V-4,5) can only be operated in the region which gives the field solution as shown in Fig. V-3c. As a consequence, they are, in general, less attractive. These guides, however, can be made to operate with a field distribution similar to Fig. V-3b inside the guide and approximately exponential behavior outside the guide by introducing sufficient dielectric loss. Marcatili (Ref. V-7) discussed the thick wall tube in this context; a similar discussion of the O-guide with dielectric loss does not appear to exist in the literature.

REFERENCES FOR SECTION V

V-1. Hondros, A. (1909). "Ann. D. Physik," 30, 905; Hondros, A., and Debye, P. (1910) "Ann. d. Physik," 32, 465.

V-2. Carson, Mead, and Schelkunoff (1936) Bell Sys. Tech. J. 15, 310.

V-3. Elsasser, W. M. (Dec. 1949) "Attenuation in a dielectric circular rod," J. Appl. Phys., vol. 20, pp. 1193-1196.

V-4. Wachowski, H. M. and Beam, R. E. (Nov. 1950) "Final report on investigation of multimode propagation in waveguides," Microwave Lab. Northwestern Univ.

V-5. Sugi, M. and Nakahara, T. (July 1959) "O-guide and X-guide: An advanced surface wave transmission concept," IRE Trans. Microwave Theory Tech., vol. MTT-7, pp. 366-369.

V-6. Snitzer, E. (May 1961) "Cylindrical dielectric waveguide modes," J. Opt. Soc. Amer. vol. 51, pp. 491-498.

V-7. Marcatili, E. A. and Schmeltzer, R. A. (July 1964) "Hollow metallic and dielectric waveguides for long distance optical transmission and laser," B.S.T.J., pp. 1783-1809.

V-8. Marcatili (Jan. 1966) "Light transmission in a multiple dielectric (gaseous and solid) guide," B.S.T.J., vol. 46, pp. 97-103.

V-9. Shojiro Kawakami and Shigeo Nishida (Dec. 1974) "Characteristics of a doubly clad optical fiber with a low indes inner cladding," IEEE J. Quant. Electr., vol. QE-10, pp. 879-887.

V-10. Kazuyaki Yamamoto (June 1980) "A novel low loss dielectric waveguide for millimeter and sub-millimeter wavelength," IEEE Trans. Microwave theory and Tech., vol. MIT-28, 6, pp. 580-584.

V-11. Waldron, R. A. (1970) "Theory of guided electromagnetic waves," Van Nostrand Reinhold Co., London, pp. 227.

DISTRIBUTION LIST - TECHNICAL REPORTS
Contract N00014-79-C-0839

Office of Naval Research 4
Code 427
Arlington, VA 22217

Naval Research Laboratory
4555 Overlook Avenue, S.W.
Washington, D.C. 20375
Attn: Code 6811 1
6850 1

Defense Logistics Agency 12
Defense Documentation Center
Bldg. 5, Cameron Station
Alexandria, VA 22314

Dr. Y. S. Park 1
AFWAL/DHR
Building 450
Wright-Patterson AFB
Ohio 45433

ERADCOM 1
DELET-M
Fort Monmouth, NJ 07703

Texas Instruments, Inc. 1
Central Research Lab
M.S. 134, P.O. Box 225936
13500 North Central Expressway
Dallas, TX 75265
Atten: Dr. Wisseman

Dr. R. M. Malbon/M.S. IC 1
Avantek, Inc.
3175 Bowers Avenue
Santa Clara, CA 94304

Mr. R. Bierig 1
Raytheon Company
28 Seyon Street
Waltham, MA 02154

Dr. R. Bell, K-101 1
Varian Associates, Inc.
611 Hansen Way
Palo Alto, CA 94304

Hewlett-Packard Corp. 1
Dr. Robert Archer
1501 Page Mill Road
Palo Alto, CA 94306

Dr. H. C. Nathanson 1
Westinghouse Research and
Development Center
Beulah Road
Pittsburgh, PA 15235

Dr. Daniel Chen 1
Rockwell International Science
Center
P.O. Box 1085
Thousand Oaks, CA 91360

Dr. D. Krumn
Hughes Research Laboratory
3011 Malibu Canyon Road
Malibu, CA 90265

Mr. Lothar Wandinger 1
ECOM/AMSEL/TL/IJ
Fort Monmouth, NJ 07003

Dr. Harry Wieder 1
Naval Ocean Systems Center
Code 922
271 Catalina Blvd.
San Diego, CA 92152

Dr. William Lindley 1
MIT
Lincoln Laboratory
F124 A, P.O. Box 73
Lexington, MA 02173

Commander 1
U.S. Army Electronics Command
V. Gelnovatch
(DRSEL-TL-IC)
Fort Monmouth, NJ 07703

RCA 1
Microwave Technology Center
Dr. F. Sterzer
Princeton, NJ 08540

Watkins-Johnson Company 1
E.J. Crescenzi, Jr./K. Niclas
3333 Hillview Avenue
Stanford Industrial Park
Palo Alto, CA 94304

Distribution List - Technical Reports (continued)

Commandant 1
Marine Corps
Scientific Advisor (Code AX)
Washington, D.C. 20380

Communications Transistor Corporation 1
Dr. W. Weisenberger
301 Industrial Way
San Carlos, CA 94070

Microwave Associates 1
Northwest Industrial Park
Drs. F. A. Brand/J. Saloom
Burlington, MA 01803

Commander, AFAL 1
AFWAL/AADM
Dr. Don Rees
Wright-Patterson AFB
Ohio 45433

Professor Walter Ku 1
Phillips Hall
Cornell University
Ithaca, NY 14853

Commander 1
Harry Diamond Laboratories
Mr. Horst W. A. Gerlach
2800 Powder Mill Road
Adelphia, MD 20783

Advisory Group on Electron Devices 1
201 Varick Street
9th Floor
New York, NY 10014

D. Claxton 1
MS/1414
TRW Systems
One Space Park
Redondo Beach, CA 90278

Professor L. Eastman 1
Phillips Hall
Cornell University
Ithaca, NY 14853

AIL TECH 1
612 N. Mary Avenue
Sunnyvale, CA 94086
Attn: G. D. Vendelin

Professors Hauser and Littlejohn 1
Department of Electrical Engr.
North Carolina State University
Raleigh, NC 27607

Professor J. Beyer 1
University of Wisconsin-Madison
750 University Avenue
Madison, Wisconsin 53706

General Electric Company 1
Attn: W. Perkins
Electronics Lab 3-115/B4
P.O. Box 4840
Syracuse, NY 13221

Professors Rosenbaum and Wolfe 1
Washington University
Semiconductor Research Laboratory
P.O. Box 1127
St. Louis, Missouri 63130

Mr. John Carson 1
Code 8212
NOSC
San Diego, CA 92152

Dr. Hans Steyskal 1
RADC/EEA
Hanscom AFB, MA 01731

Dr. Richard Brandt 2
ONR WEST
1030 E. Green Street
Pasadena, CA 91106

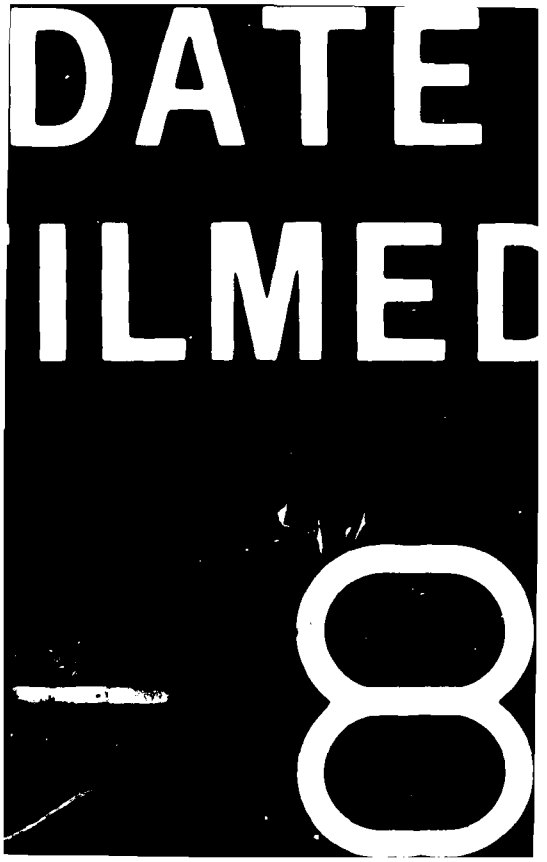
DATE
ILMED
8